



# Measurement of the deuteron coalescence probability in jets with ALICE

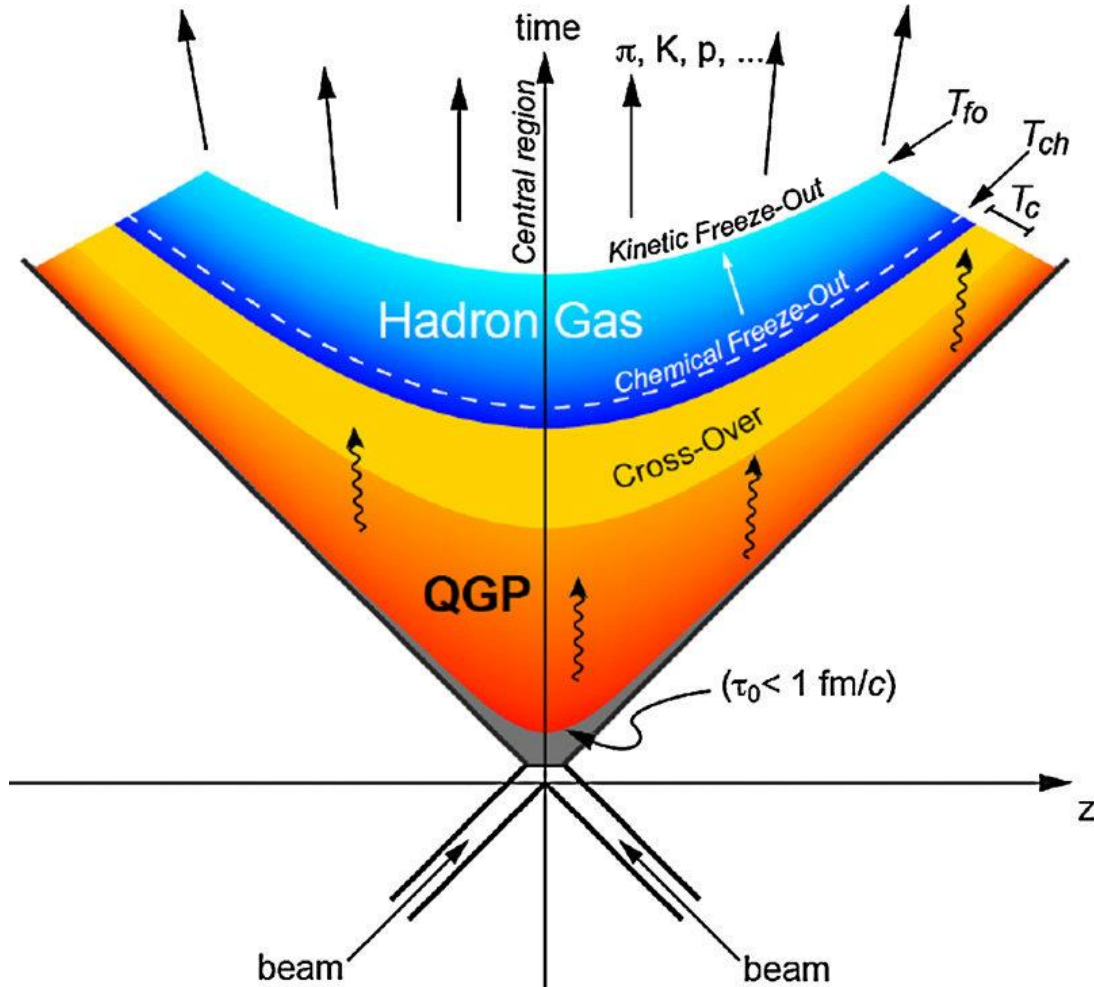
Marika Rasà\*

On behalf of the ALICE Collaboration

\*University and INFN of Catania



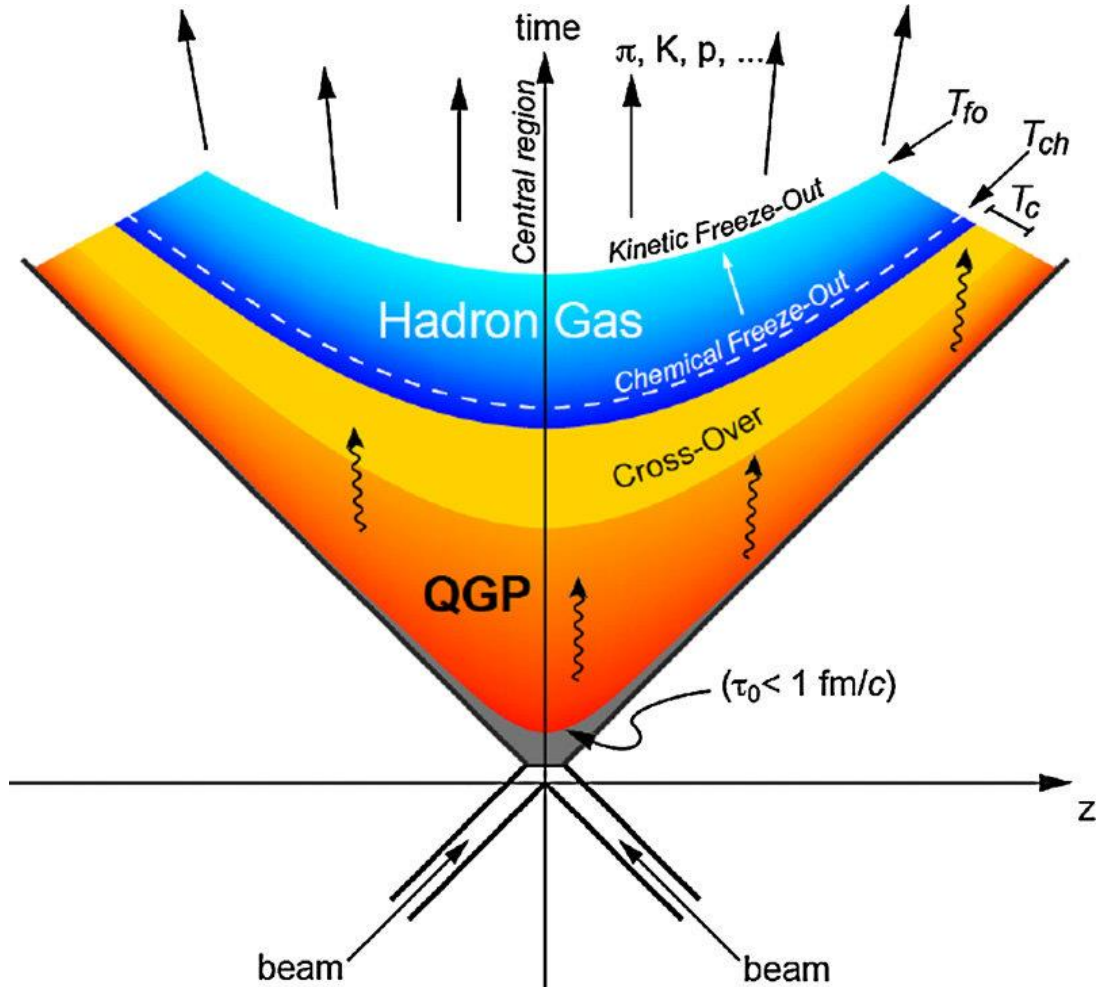
# Physics motivation



- Light (anti)nuclei are produced in high-energy hadronic collisions at the LHC
- Matter and antimatter are produced in (almost) the same amount at midrapidity
- Their production mechanism is still not understood
- Two phenomenological models:
  - Statistical hadronization
  - Coalescence



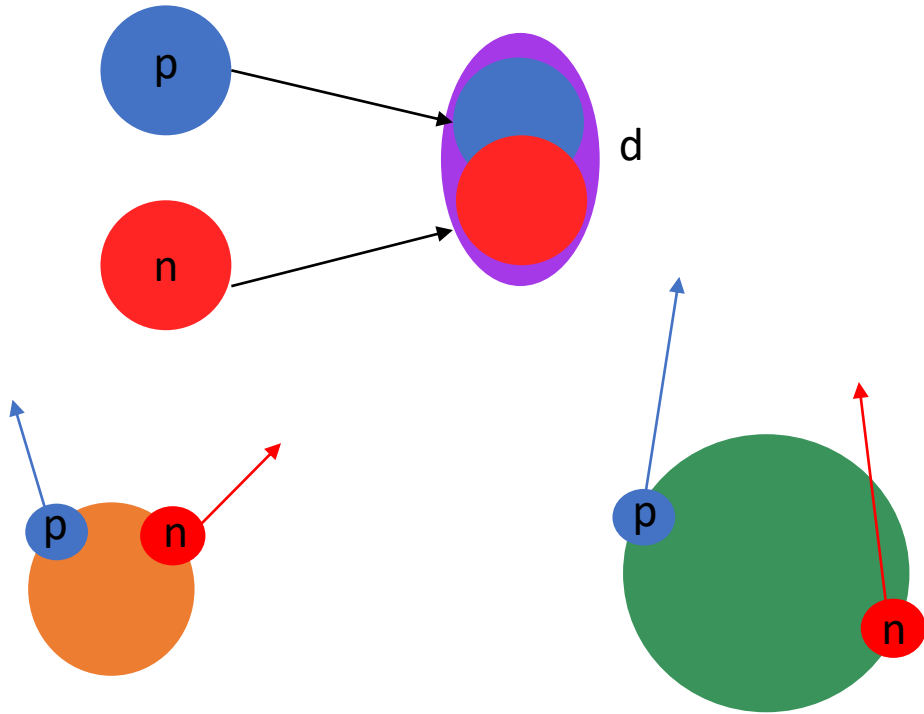
# Physics motivation



- Light (anti)nuclei are produced in high-energy hadronic collisions at the LHC
- Matter and antimatter are produced in (almost) the same amount at midrapidity
- Their production mechanism is still not understood
- Two phenomenological models:
  - Statistical hadronization
  - Coalescence *Focus on it*

# Coalescence model

S. T. Butler et al., Phys. Rev. 129 (1963) 836



Small source size  $\rightarrow$  Large  $B_A$   
 $pp \sim 1$  fm  
 $p\text{-Pb} \sim 1.5$  fm

Large source size  $\rightarrow$  Small  $B_A$   
 $\text{Pb-Pb} \sim 3\text{-}6$  fm

- If (anti)nucleons are close in phase space and match the spin state, they can form an (anti)nucleus
- Coalescence parameter  $B_A$  is the key observable:

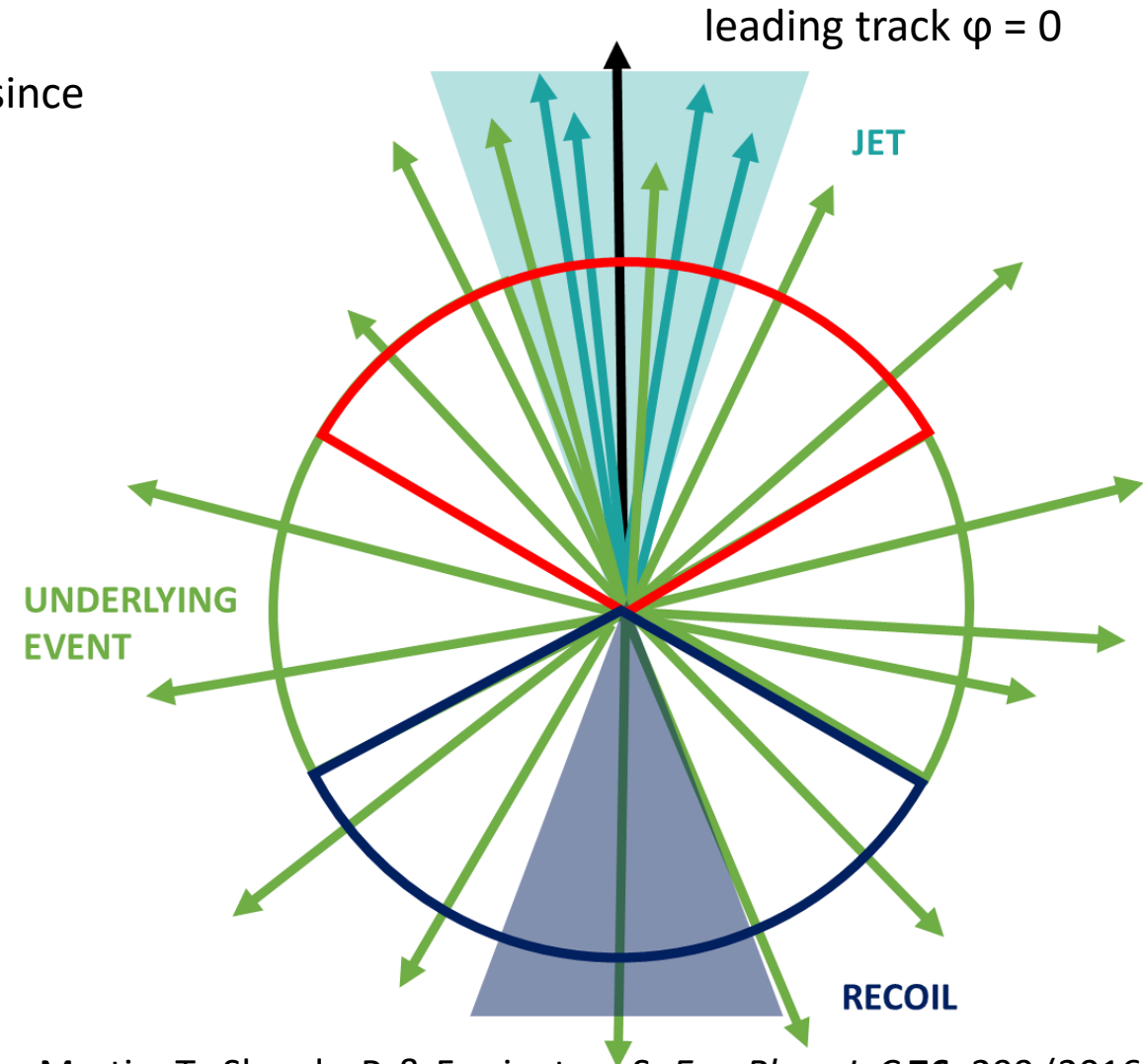
$$E_A \frac{d^3 N_A}{dp_A^3} = B_A \cdot \left( E_p \frac{d^3 N_p}{dp_p^3} \right)^A \quad p_p = p_A/A$$

Invariant yield of nucleus      Coalescence parameter      Invariant yield of protons

- Coalescence parameter depends on both the source size and radial extension of the nucleus wave function:

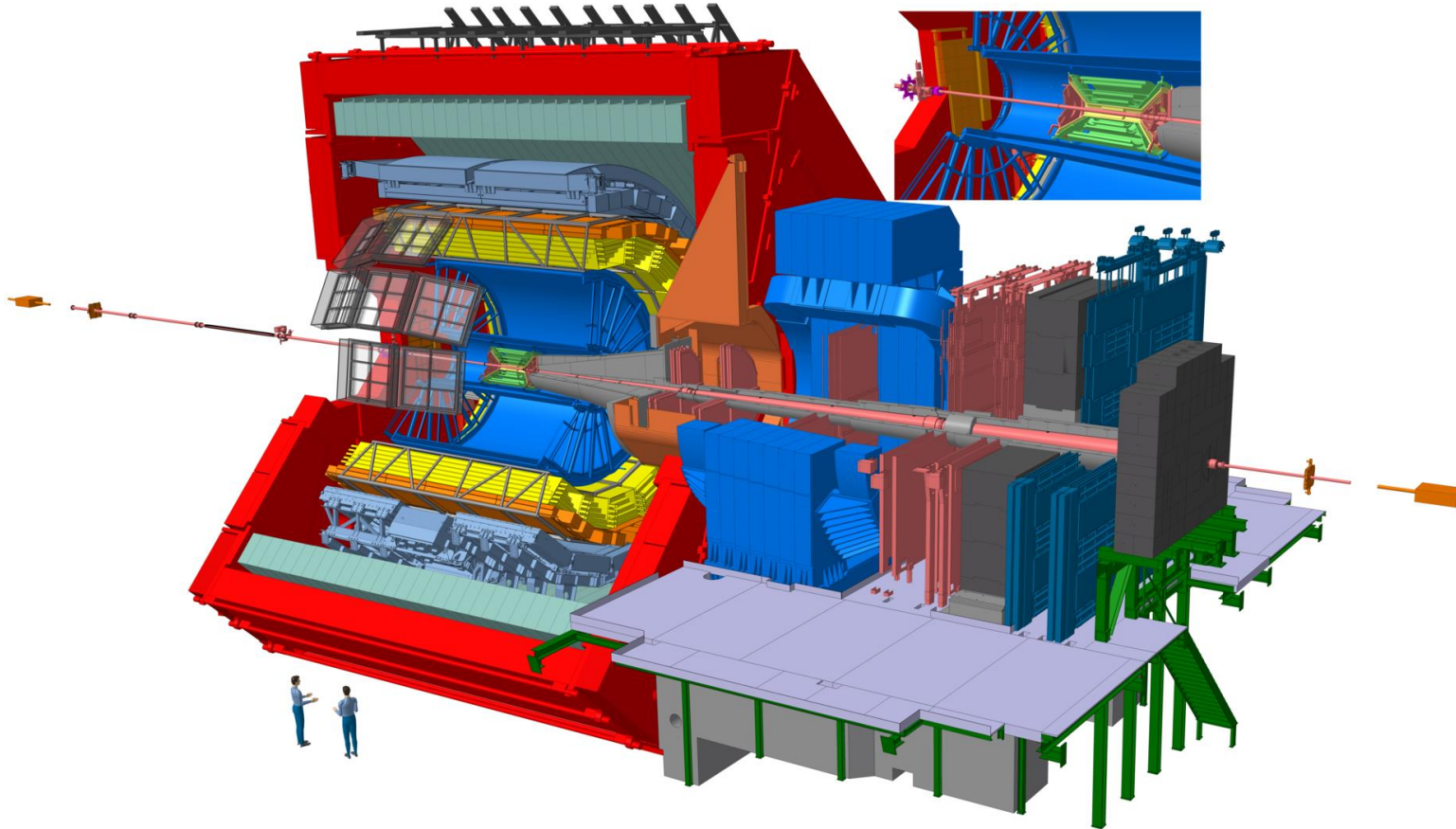
# In-jet and underlying event

- The study in small systems, such as pp and p–Pb, is interesting since the nucleons are closer in phase space wrt Pb–Pb
- Leading particle (highest  $p_T$  and  $p_T > 5 \text{ GeV}/c$ ) used as a proxy for the jet axis
- CDF technique used to find the three azimuthal regions
  - **Toward** ( $|\Delta\phi| < 60^\circ$ ) : contains JET and UE
  - **Transverse** ( $60^\circ < |\Delta\phi| < 120^\circ$ ) : dominated by the Underlying Event (UE)
  - **Away** ( $|\Delta\phi| > 120^\circ$ ): contains recoil jet and UE
- **Jet: Toward – Transverse**



Martin, T., Skands, P. & Farrington, S. *Eur. Phys. J. C* **76**, 299 (2016)

# The ALICE detector in Run 2

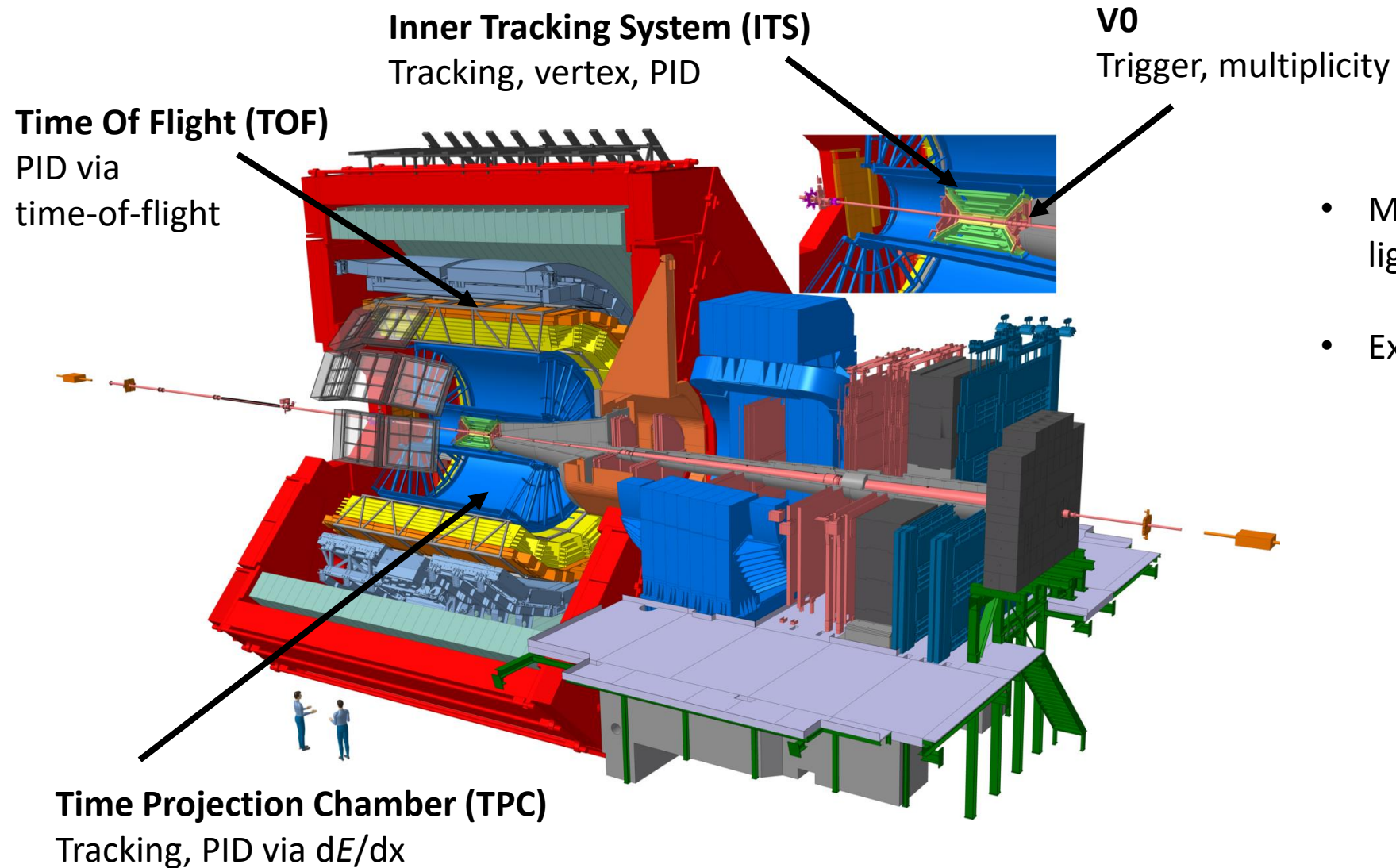


- Most suited LHC experiment to study light (anti)nuclei production
- Excellent PID capabilities

*JINST* 3 (2008) S08002

Int. J. Mod. Phys. A 29 (2014) 1430044

# The ALICE detector in Run 2



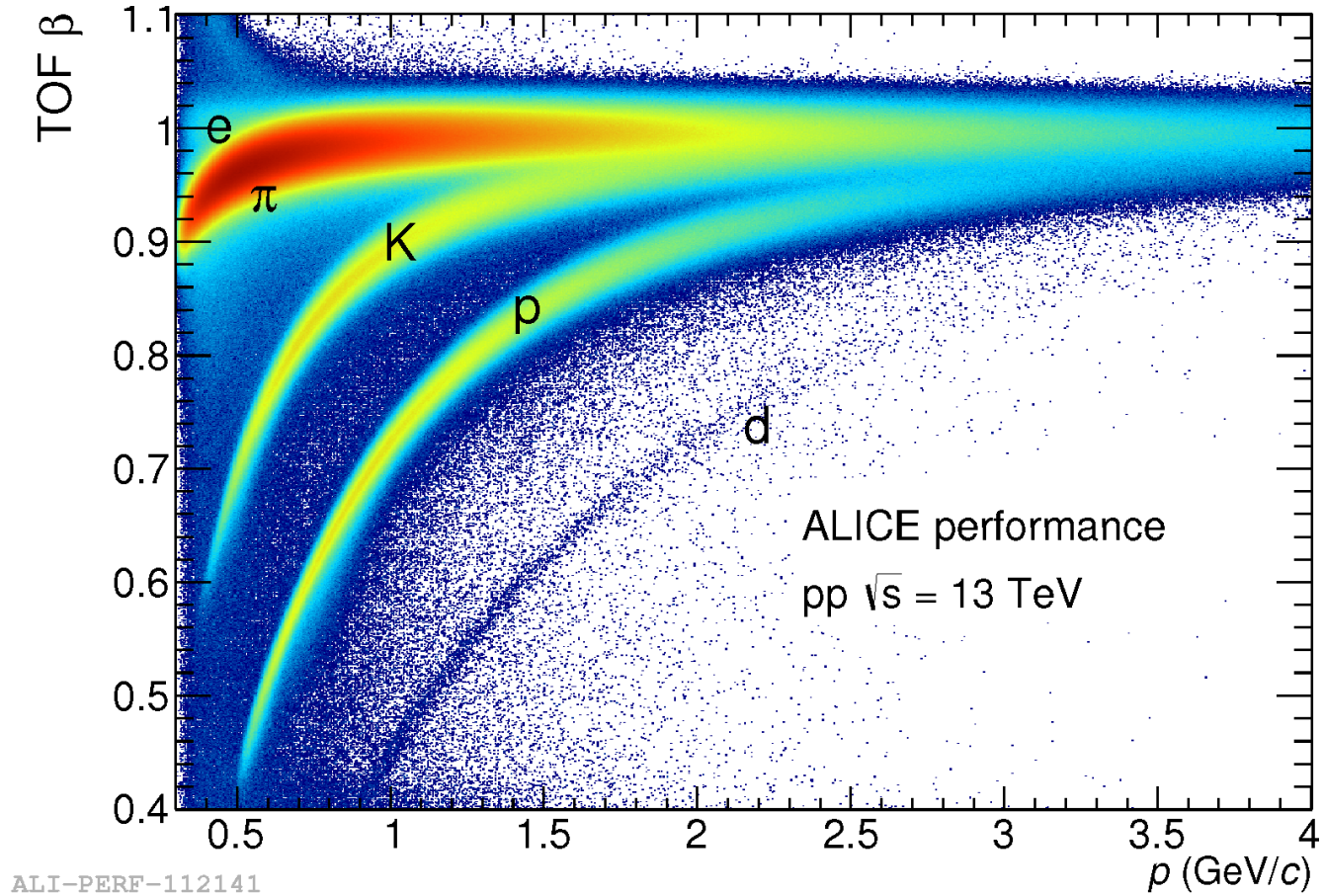
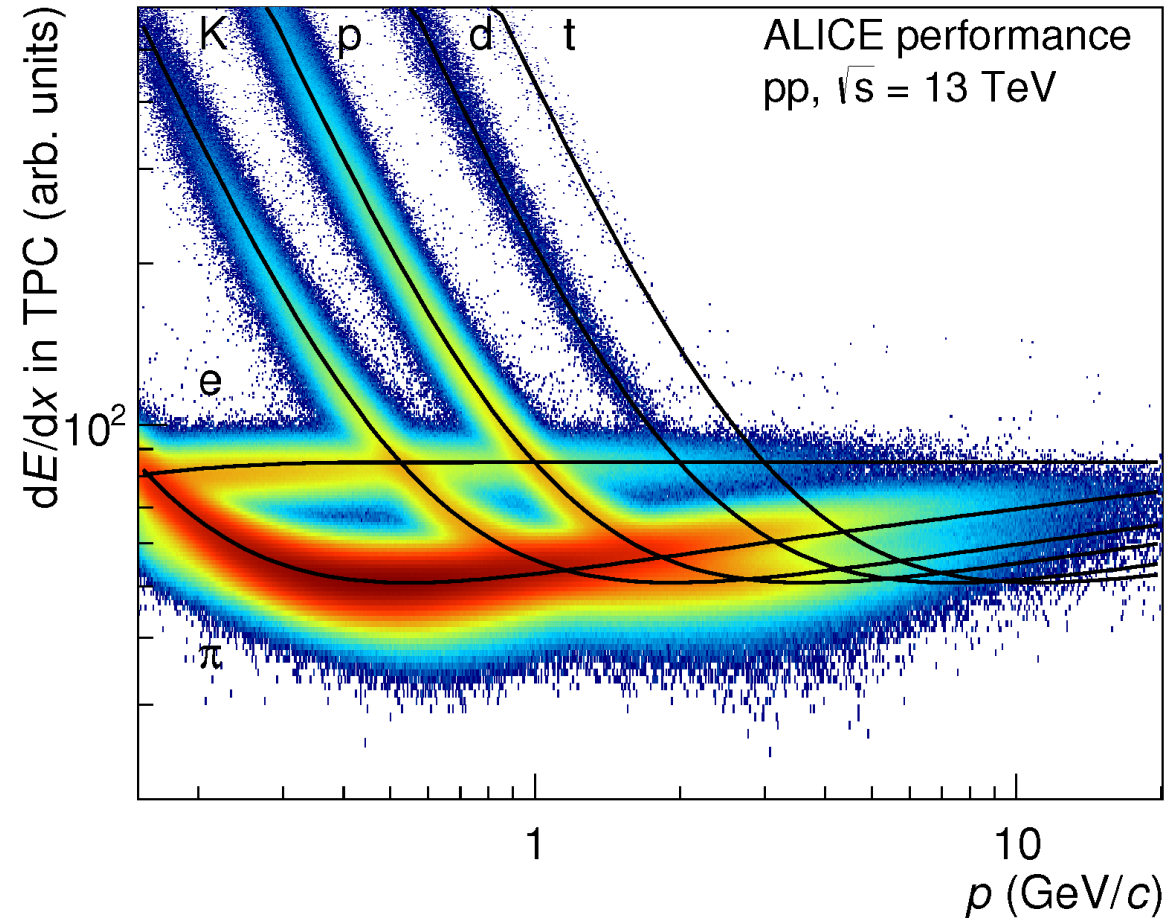
- Most suited LHC experiment to study light (anti)nuclei production
- Excellent PID capabilities

*JINST* 3 (2008) S08002

Int. J. Mod. Phys. A 29 (2014) 1430044



# Deuteron identification



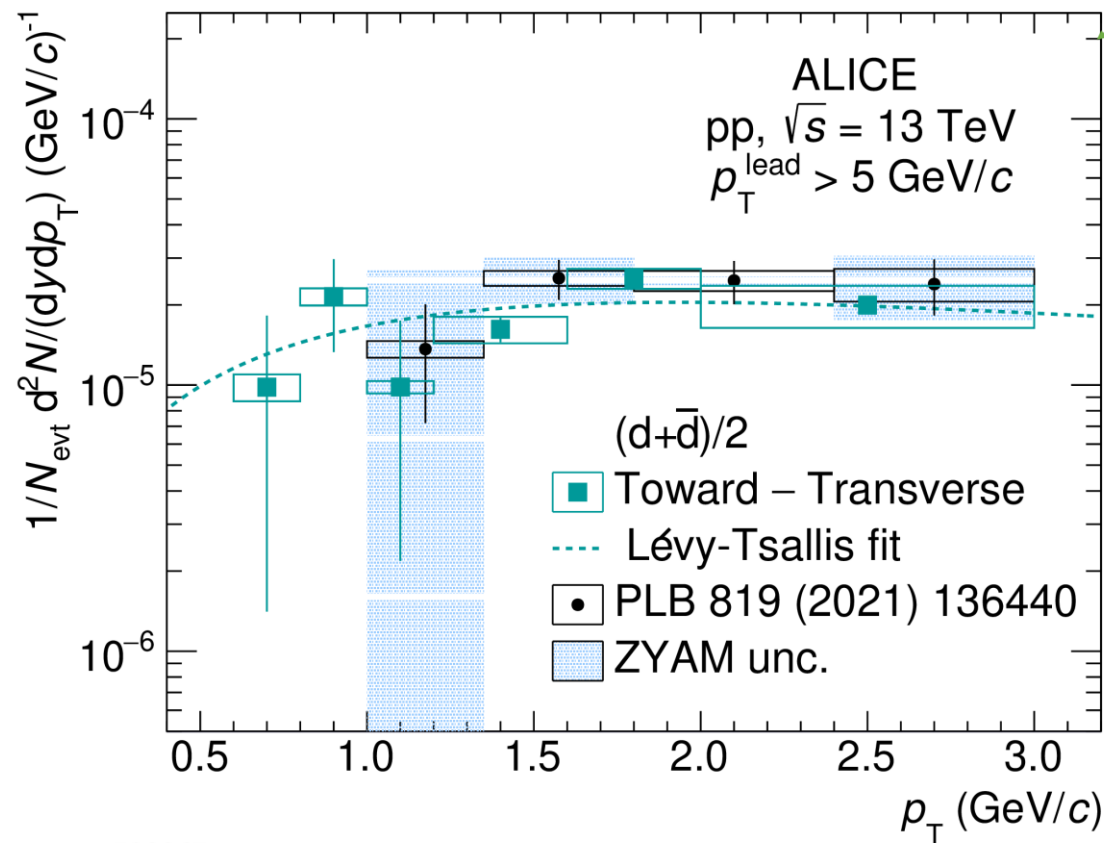
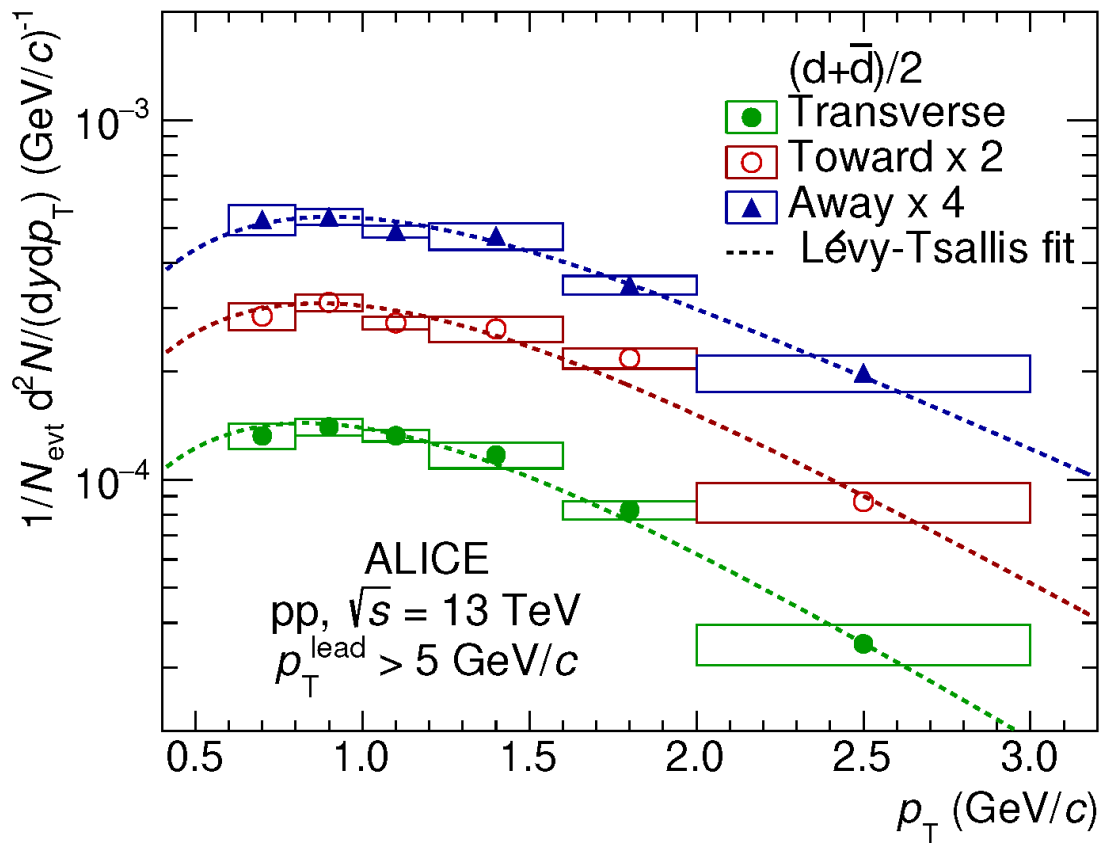
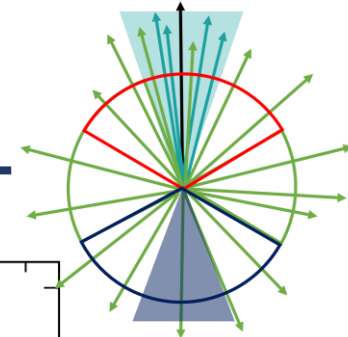
ALI-PERF-112141

Low  $p_T$  region (below 1 GeV/c): PID via  $dE/dx$   
 $\sigma_{dE/dx} \sim 5.5\%$  in pp,  $\sim 7\%$  in Pb-Pb

High  $p_T$  region (over 1 GeV/c): PID via time-of-flight  
 $\sigma_{PID} \sim 70$  ps for pp,  $\sim 60$  ps for Pb-Pb



# (Anti)deuteron spectra: pp @ 13 TeV



Jet = Toward – Transverse

ALI-PUB-533063

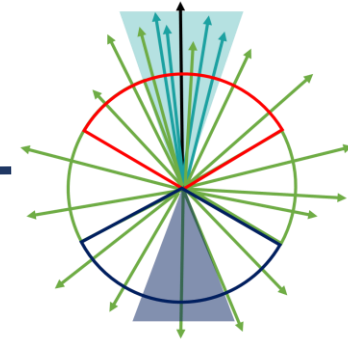
arXiv:2211.15204v1

ALI-PUB-533067

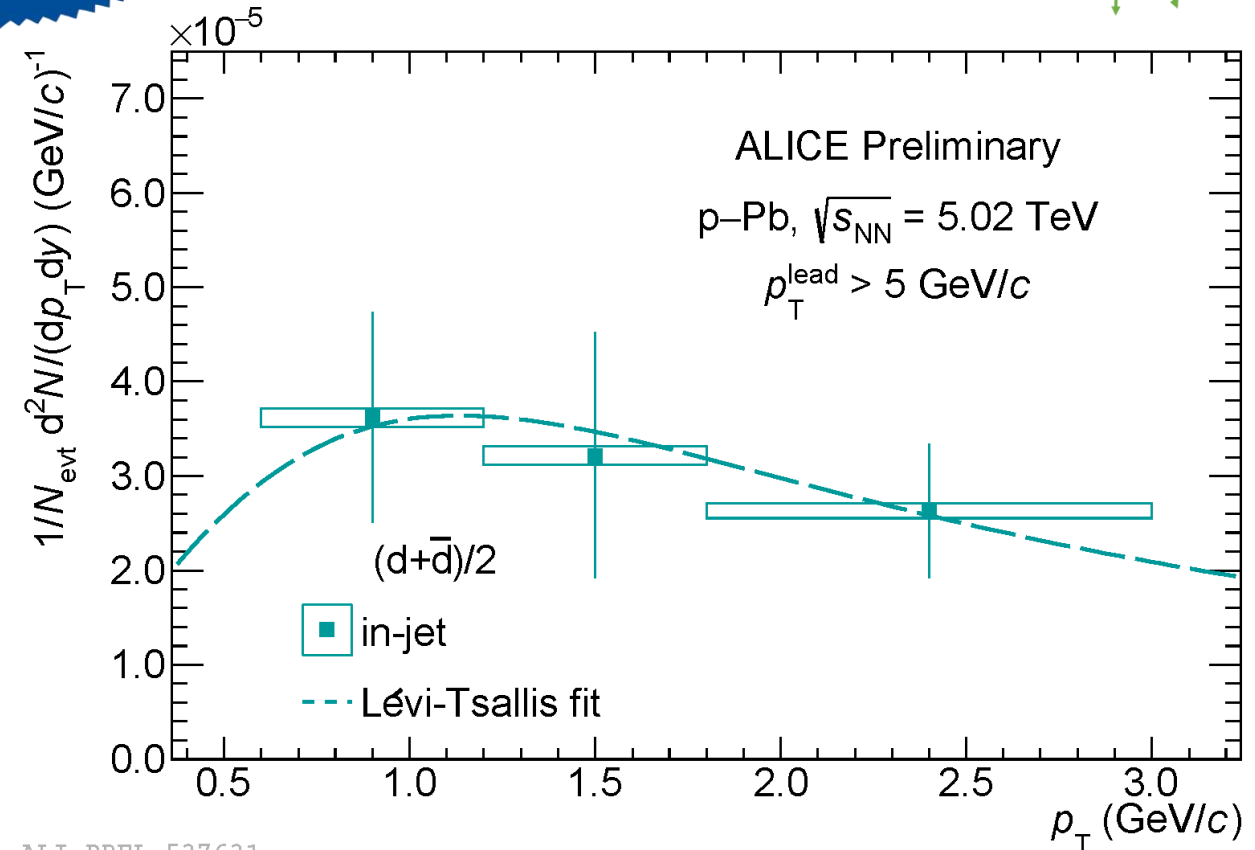
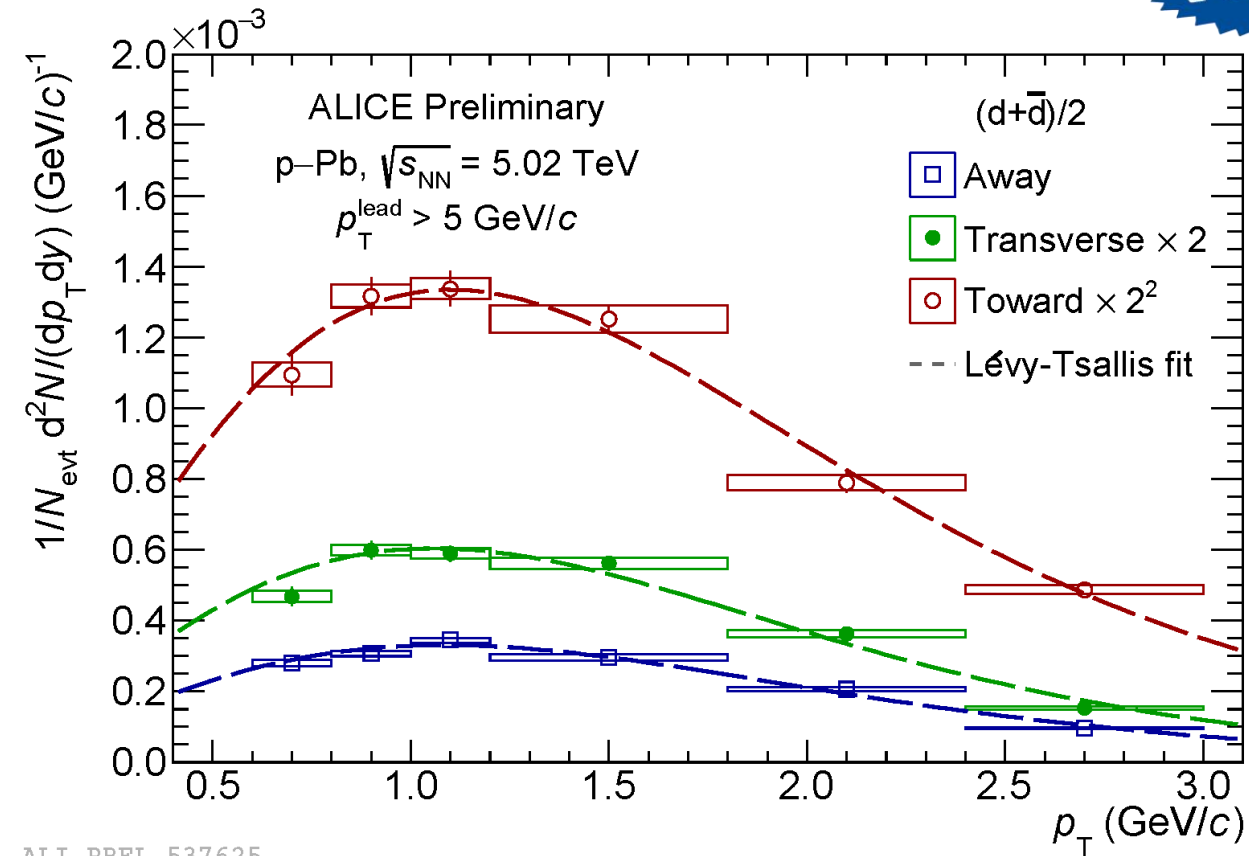
Deuteron production in events with  $p_T^{\text{lead}} > 5$  GeV/c

The results are consistent with those obtained using the two-particle correlation method

# (Anti)deuteron spectra: p-Pb @ 5.02 TeV



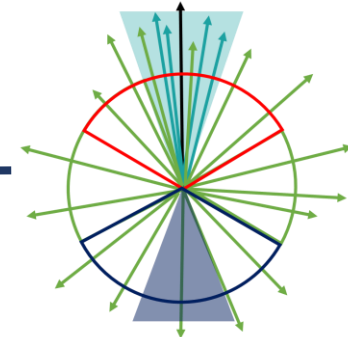
**NEW!**



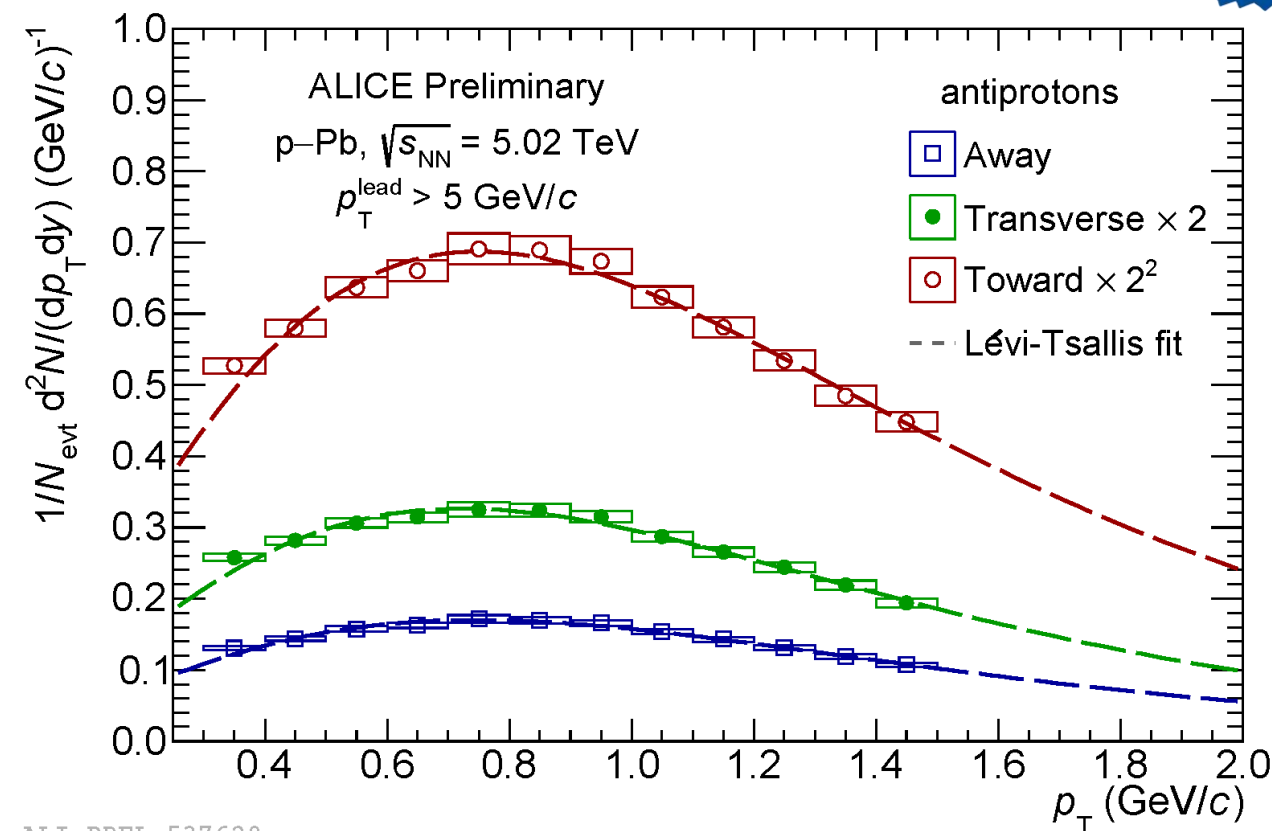
Deuteron production in events with  $p_T^{\text{lead}} > 5$  GeV/c

Jet = Toward - Transverse

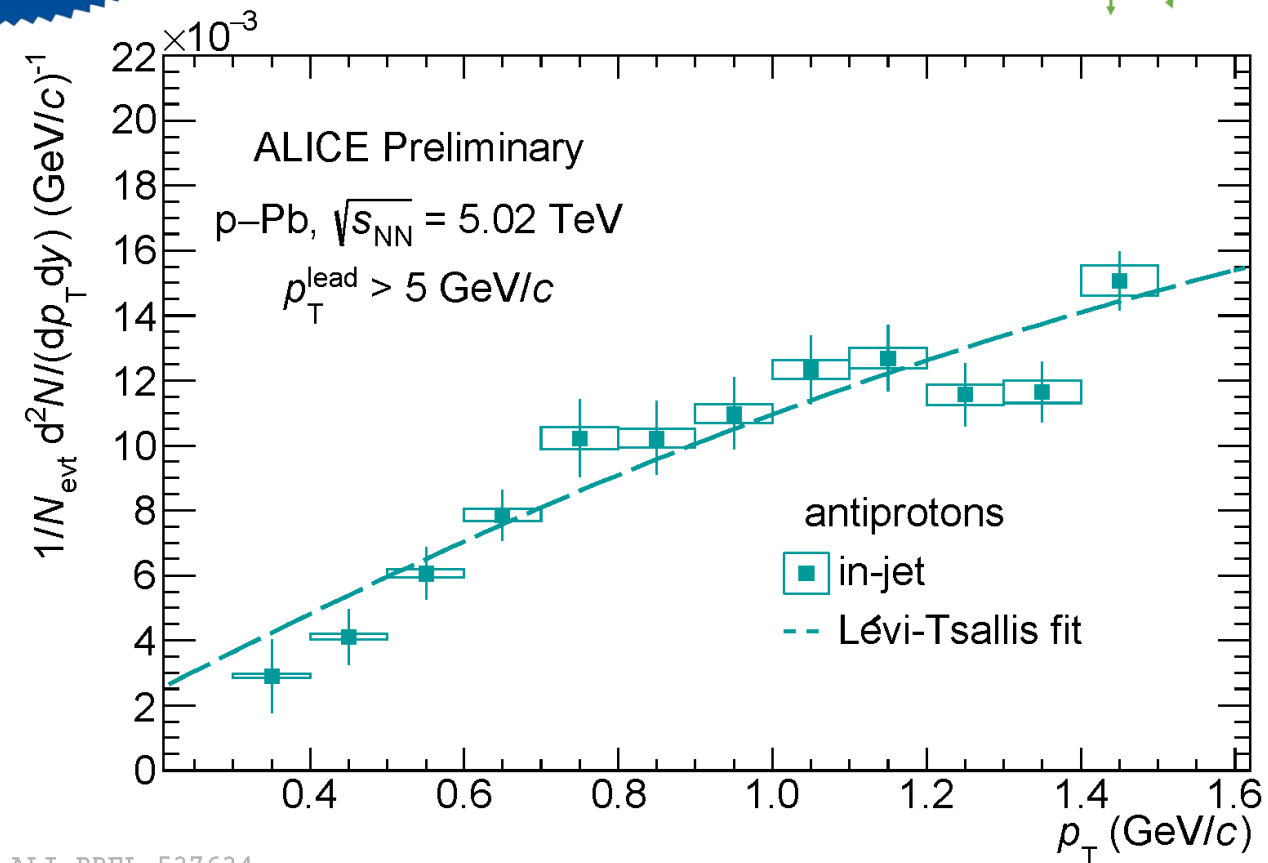
# Antiproton spectra: p–Pb @ 5.02 TeV



**NEW!**



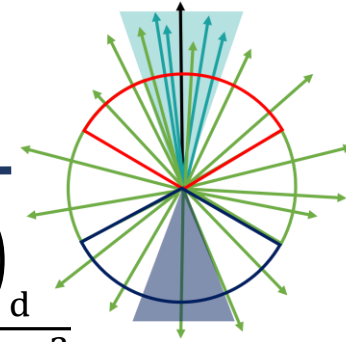
Antiproton production in events with  $p_T^{\text{lead}} > 5$  GeV/c



Jet = Toward - Transverse

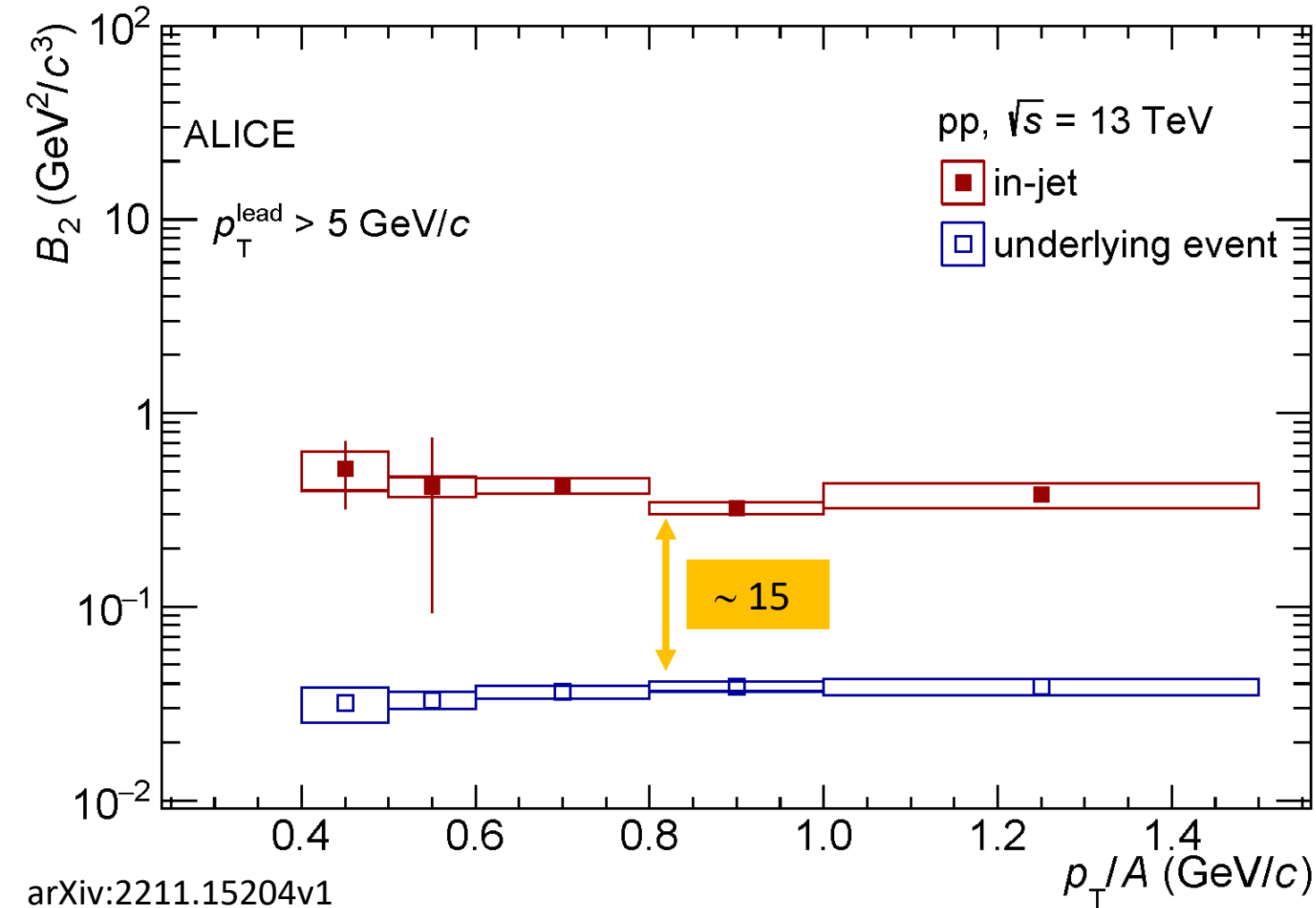


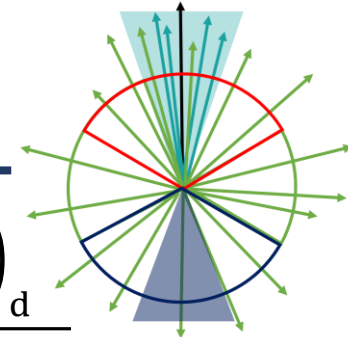
# $B_2$ in jet and UE



$$B_2 = \frac{\frac{1}{(2\pi/3)p_T^d} \left( \frac{d^2N}{dydp_T} \right)_d}{\left( \frac{1}{(2\pi/3)p_T^p} \left( \frac{d^2N}{dydp_T} \right)_p \right)^2}$$

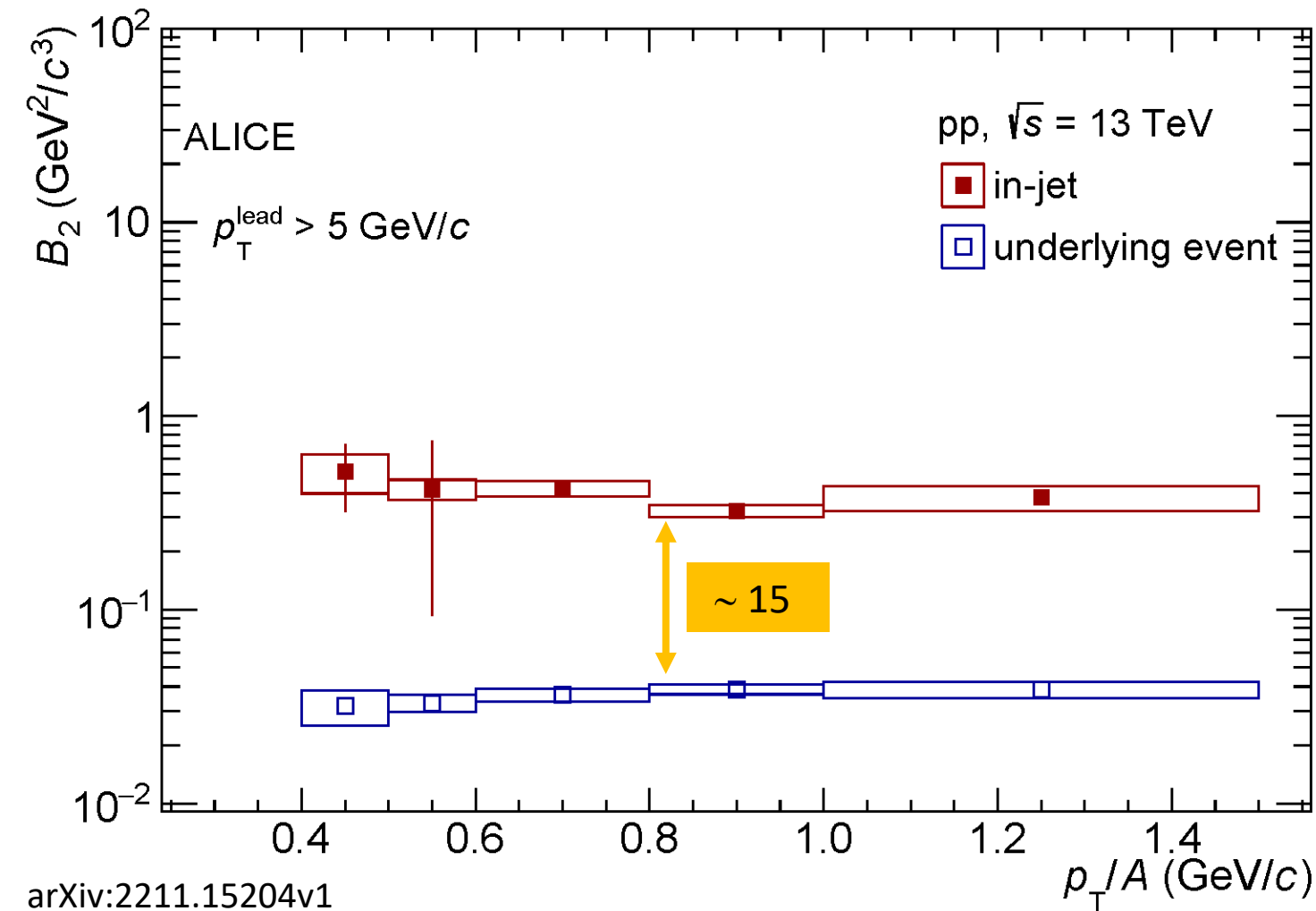
- Enhancement of  $B_2^{\text{jet}}$  wrt  $B_2^{\text{UE}}$  in pp collisions

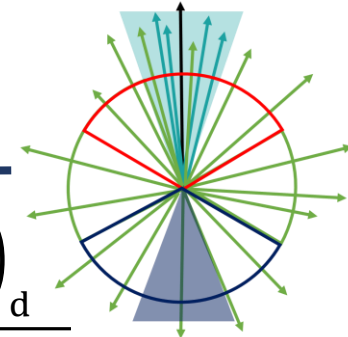




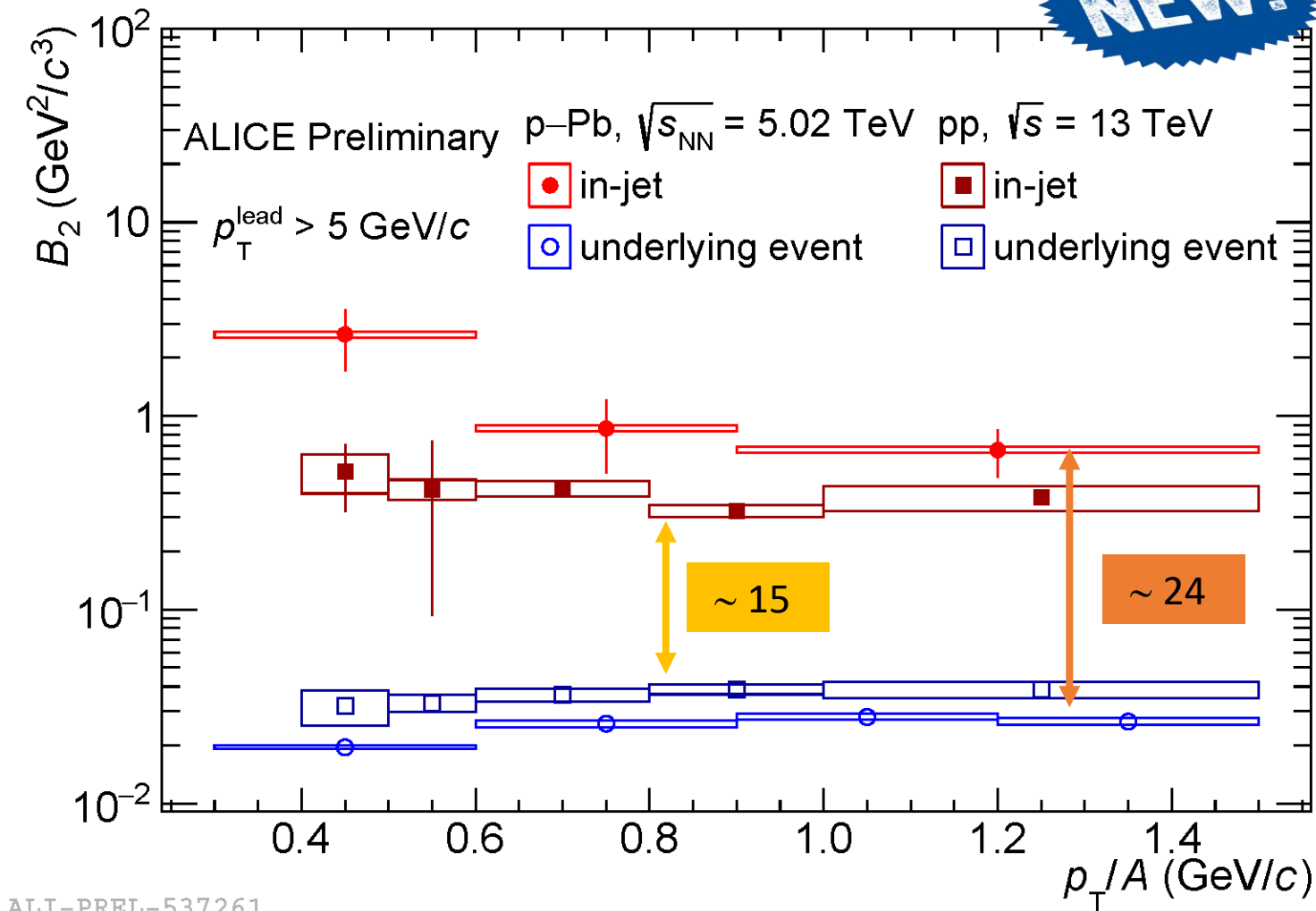
$$B_2 = \frac{\frac{1}{(2\pi/3)p_T^d} \left( \frac{d^2N}{dydp_T} \right)_d}{\left( \frac{1}{(2\pi/3)p_T^p} \left( \frac{d^2N}{dydp_T} \right)_p \right)^2}$$

- Enhancement of  $B_2^{\text{jet}}$  wrt  $B_2^{\text{UE}}$  in pp collisions
- What happens in p-Pb collisions?





**NEW!**

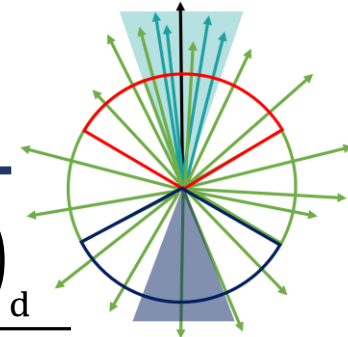


$$B_2 = \frac{\frac{1}{(2\pi/3)p_T^d} \left( \frac{d^2N}{dydp_T} \right)_d}{\left( \frac{1}{(2\pi/3)p_T^p} \left( \frac{d^2N}{dydp_T} \right)_p \right)^2}$$

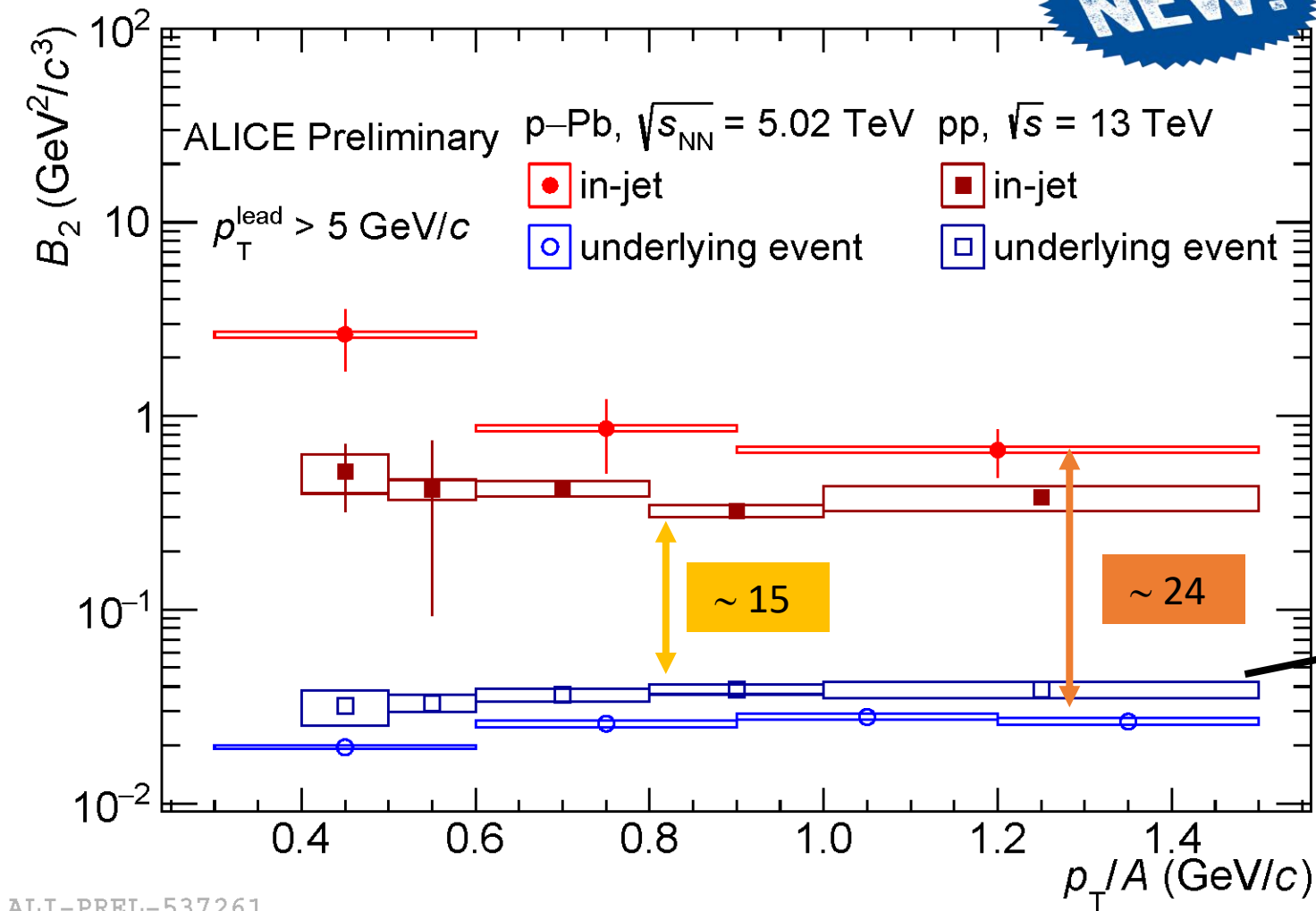
- Enhancement of  $B_2^{\text{jet}}$  wrt  $B_2^{\text{UE}}$  in pp collisions
- What happens in p-Pb collisions?
- Enhancement factor is larger wrt pp collisions



# $B_2$ in jet and UE



**NEW!**

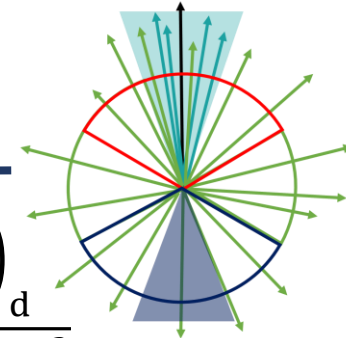


$$B_2 = \frac{\frac{1}{(2\pi/3)p_T^d} \left( \frac{d^2N}{dydp_T} \right)_d}{\left( \frac{1}{(2\pi/3)p_T^p} \left( \frac{d^2N}{dydp_T} \right)_p \right)^2}$$

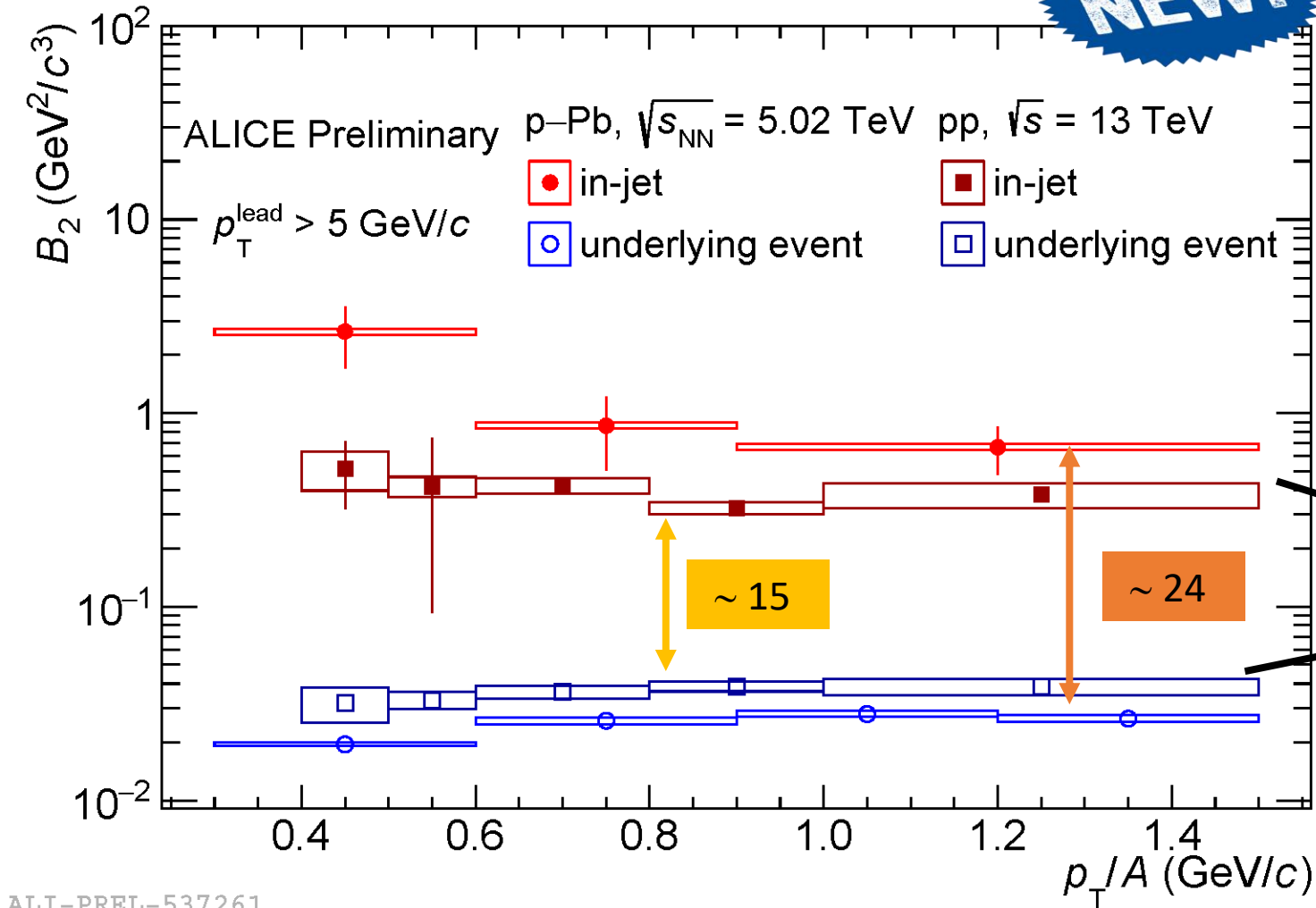
- Enhancement of  $B_2^{\text{jet}}$  wrt  $B_2^{\text{UE}}$  in pp collisions
- What happens in  $p$ -Pb collisions?
- Enhancement factor is larger wrt pp collisions

$B_2^{\text{UE}}(p\text{-Pb}) < B_2^{\text{UE}}(pp)$  since  $p$ -Pb source size is larger than pp source size

# $B_2$ in jet and UE



**NEW!**



$$B_2 = \frac{\frac{1}{(2\pi/3)p_T^d} \left( \frac{d^2N}{dy dp_T} \right)_d}{\left( \frac{1}{(2\pi/3)p_T^p} \left( \frac{d^2N}{dy dp_T} \right)_p \right)^2}$$

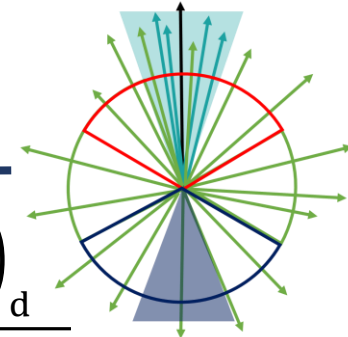
- Enhancement of  $B_2^{\text{jet}}$  wrt  $B_2^{\text{UE}}$  in pp collisions
- What happens in p-Pb collisions?
- Enhancement factor is larger wrt pp collisions

$B_2^{\text{jet}}(p\text{-Pb}) > B_2^{\text{jet}}(pp)$

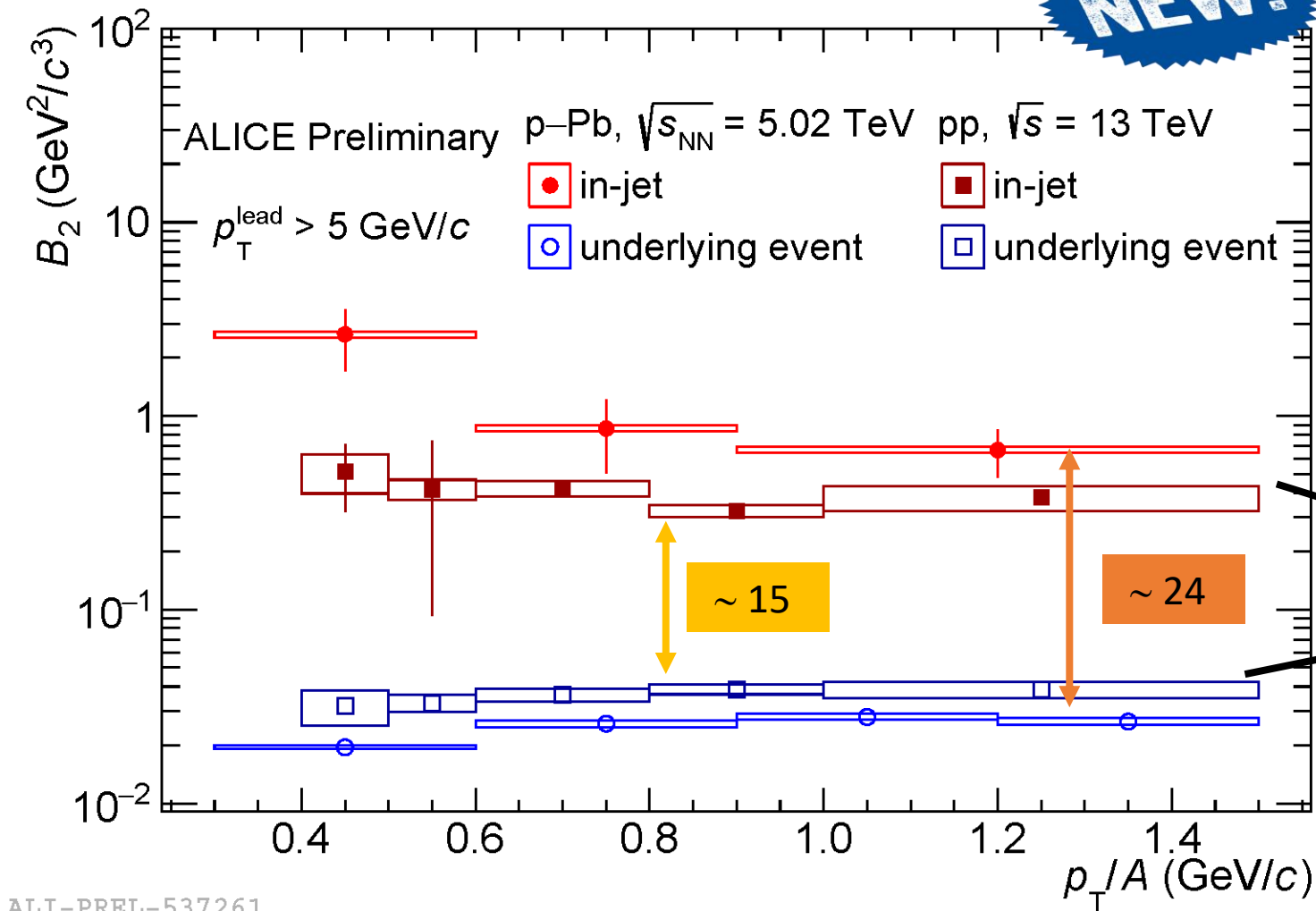
$B_2^{\text{UE}}(p\text{-Pb}) < B_2^{\text{UE}}(pp)$  since p-Pb source size is larger than pp source size

**Assuming the same source size for nucleons in jet, nucleons are probably closer in momentum space in p-Pb wrt pp**

# $B_2$ in jet and UE



**NEW!**



$$B_2 = \frac{\frac{1}{(2\pi/3)p_T^d} \left( \frac{d^2N}{dydp_T} \right)_d}{\left( \frac{1}{(2\pi/3)p_T^p} \left( \frac{d^2N}{dydp_T} \right)_p \right)^2}$$

- Enhancement of  $B_2^{\text{jet}}$  wrt  $B_2^{\text{UE}}$  in pp collisions
- What happens in p-Pb collisions?
- Enhancement factor is larger wrt pp collisions

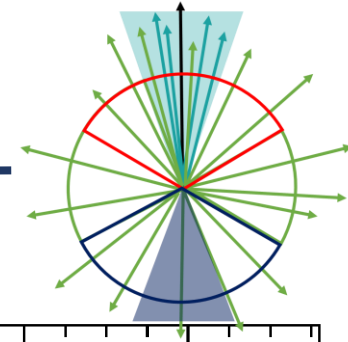
**$B_2^{\text{jet}}(p\text{-Pb}) > B_2^{\text{jet}}(pp)$**

$B_2^{\text{UE}}(p\text{-Pb}) < B_2^{\text{UE}}(pp)$  since p-Pb source size is larger than pp source size

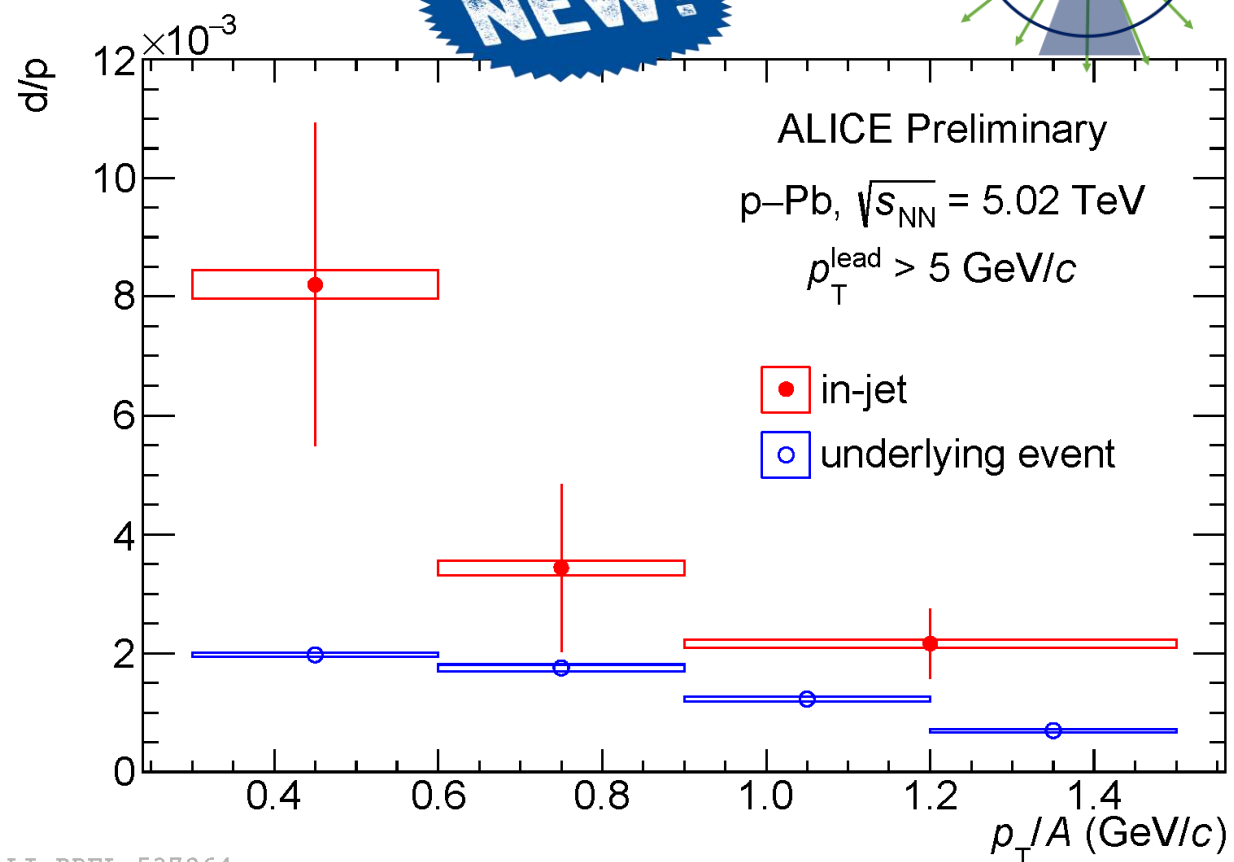
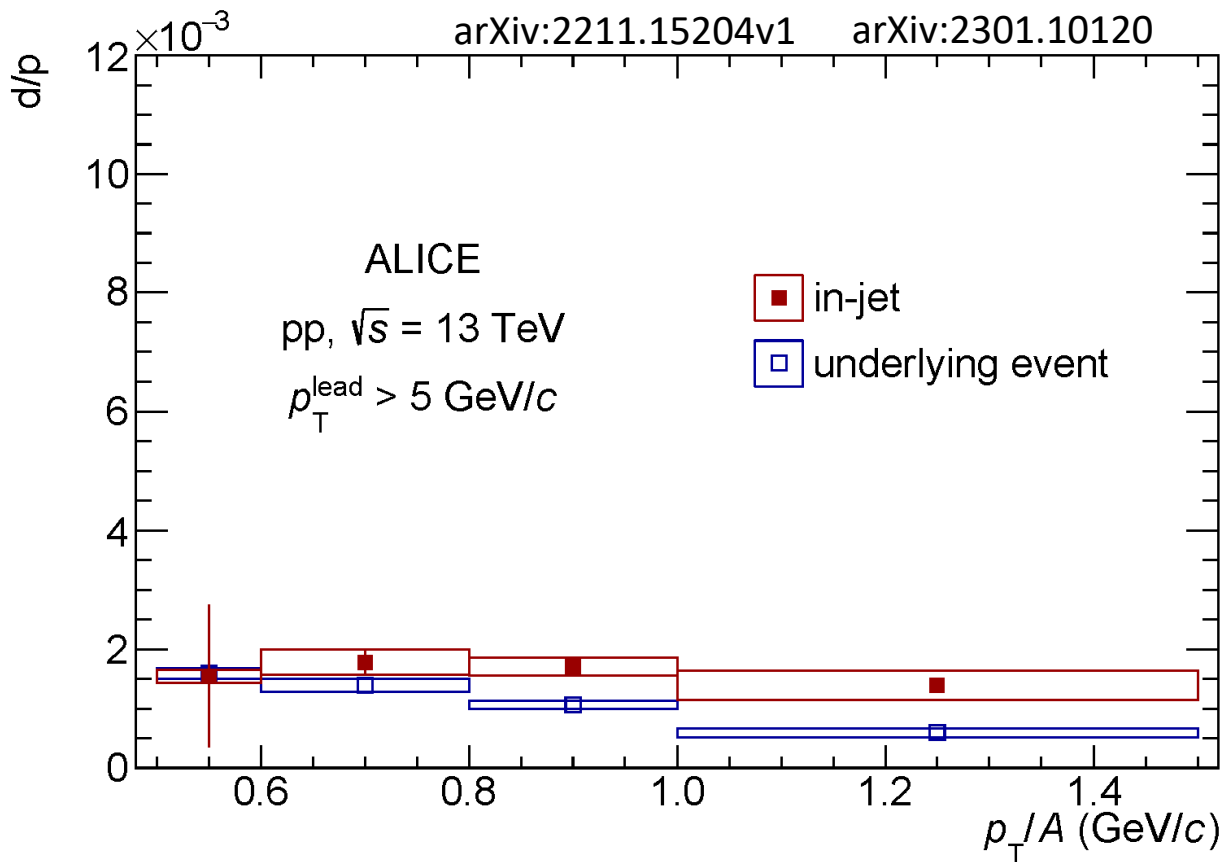
**For the first time, we see some differences between jets in pp and p-Pb collisions**

**Difference related to particle composition?**





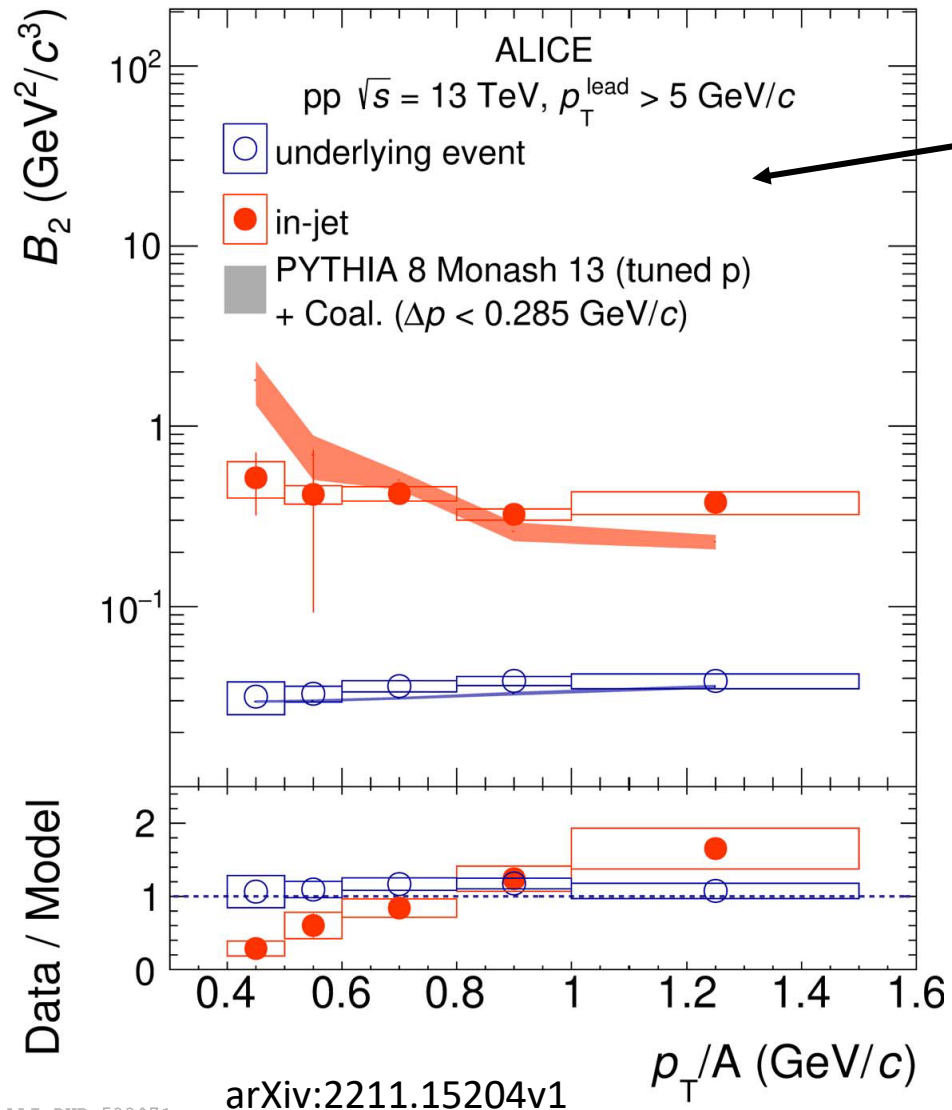
**NEW!**



ALI-PREL-537264

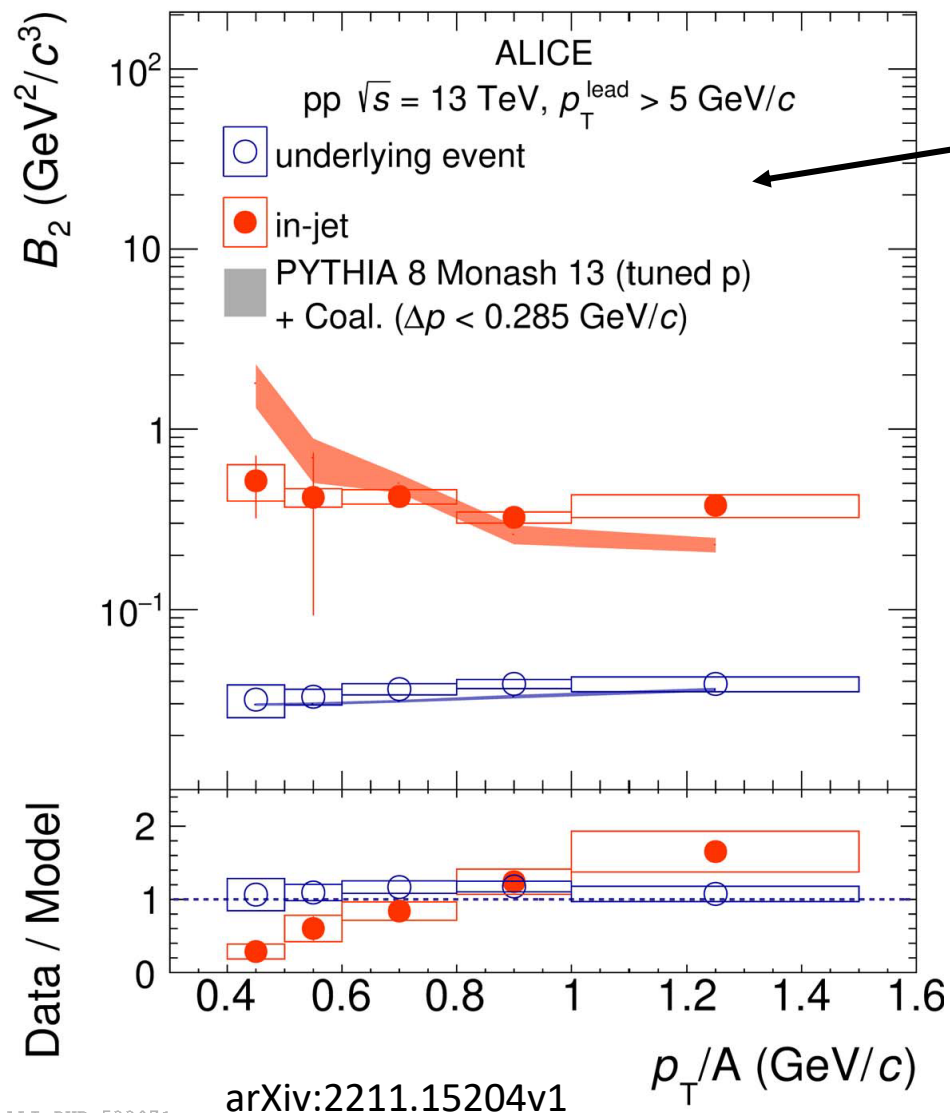
- d/p calculated as ratio of normalized spectra
- d/p<sup>jet</sup> is higher than d/p<sup>UE</sup>
- Higher d/p<sup>jet</sup> in p-Pb collisions wrt pp collisions**
- Different particle composition → could affect the coalescence probability

# $B_2$ in jet and UE – model comparison

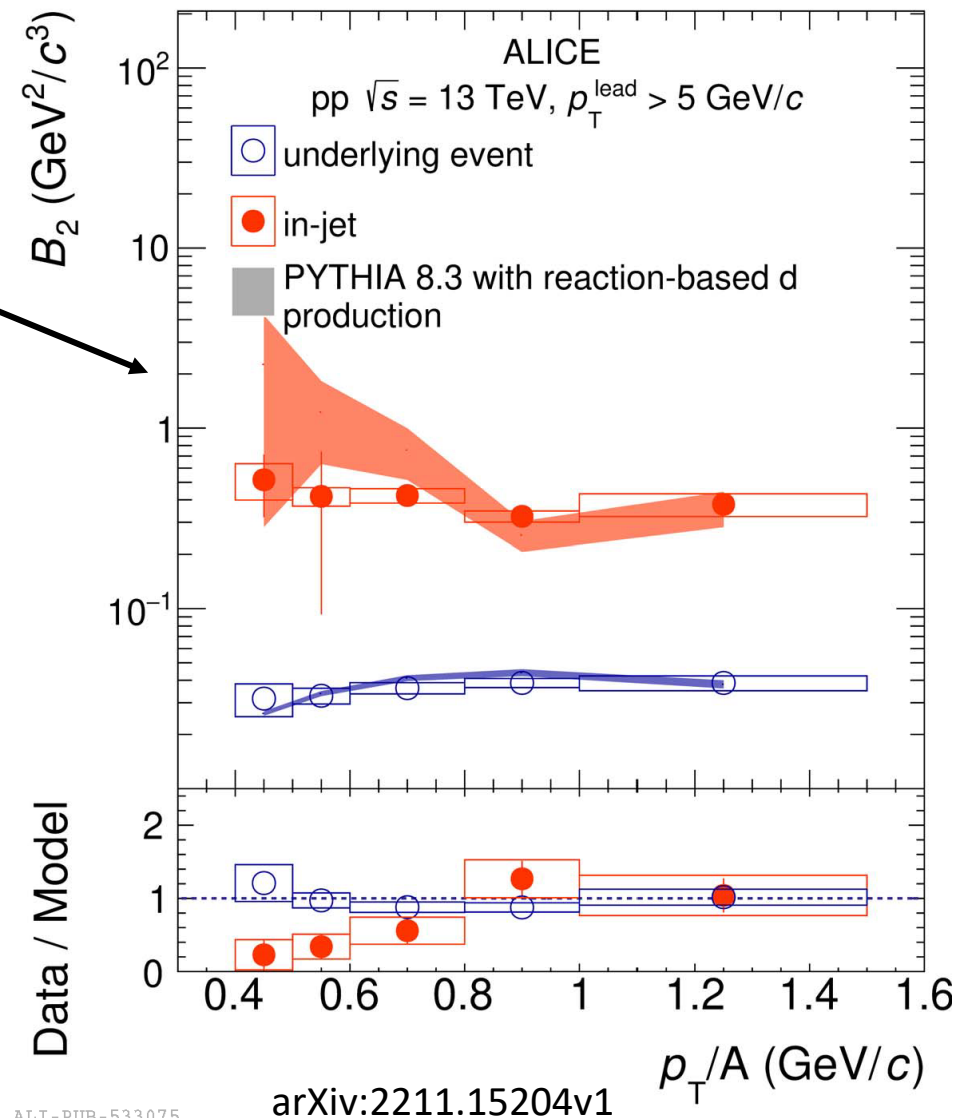


- Two different models:
  - PYTHIA 8 Monash 13 + simple coalescence

# $B_2$ in jet and UE – model comparison

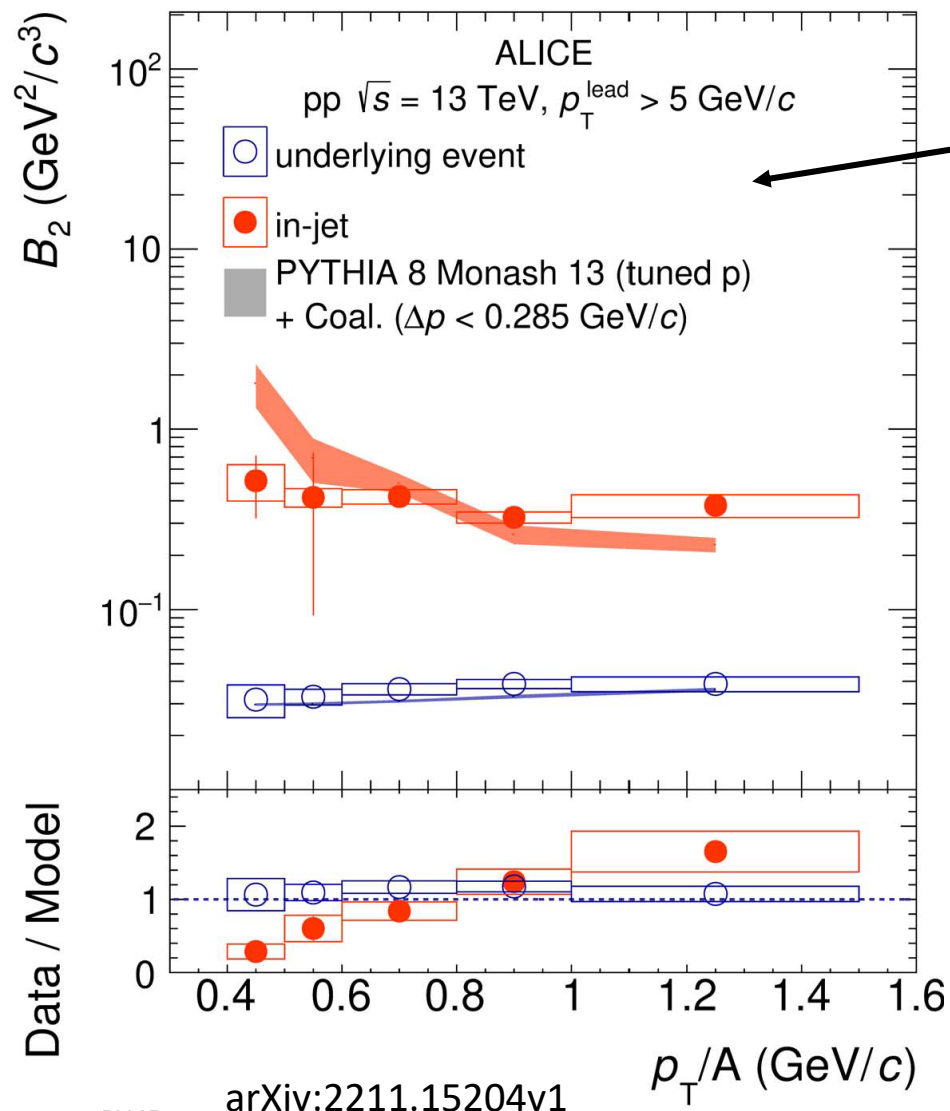


- Two different models:
  - PYTHIA 8 Monash 13 + simple coalescence
  - PYTHIA 8.3 with reaction-based deuteron production (Bierlich et al., arXiv:2203.11601)

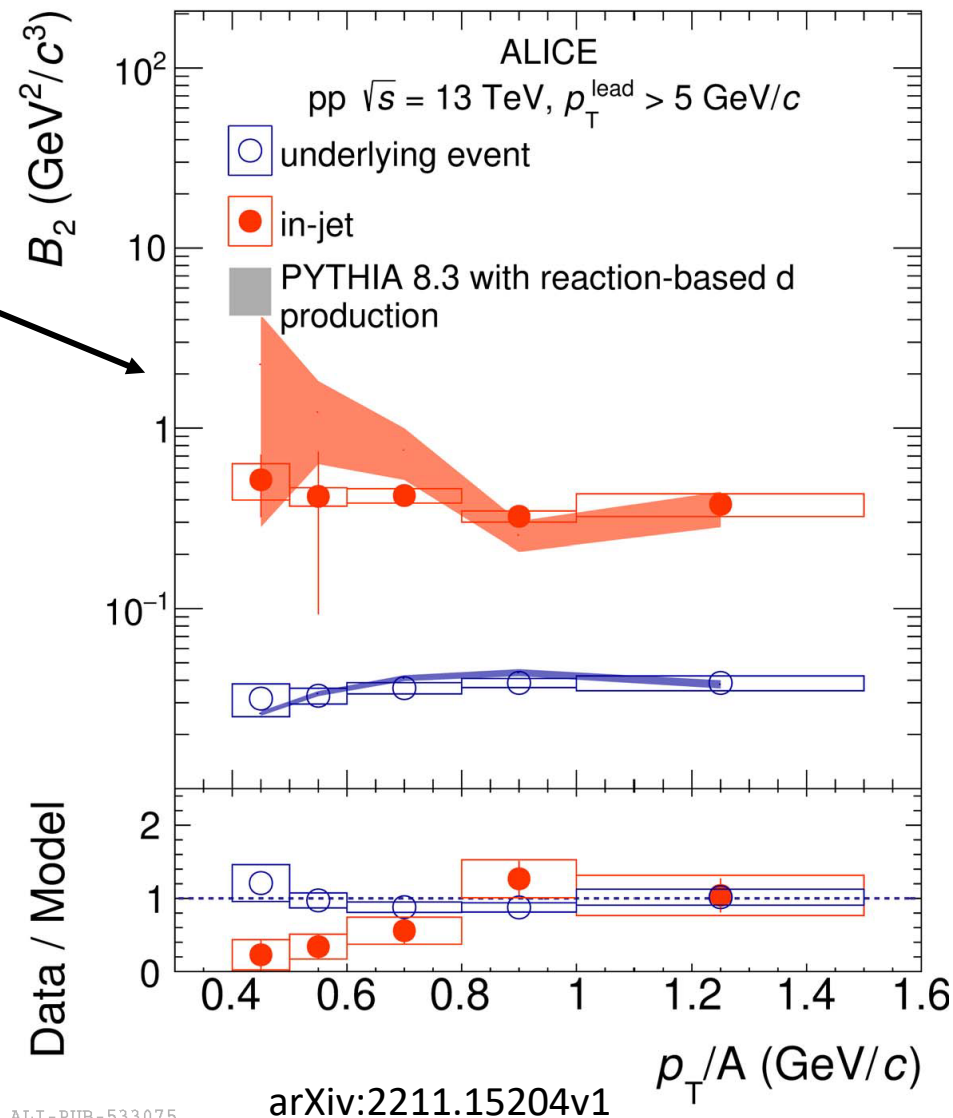




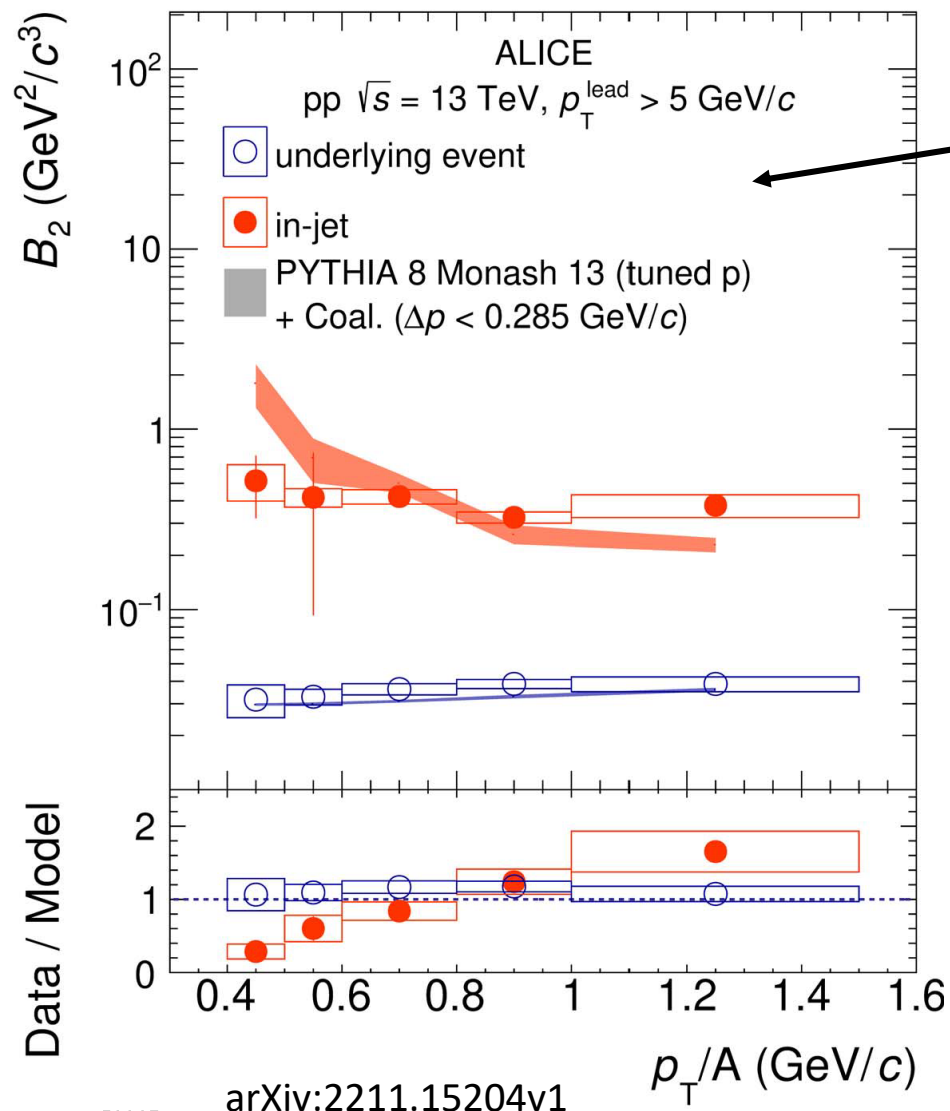
# $B_2$ in jet and UE – model comparison



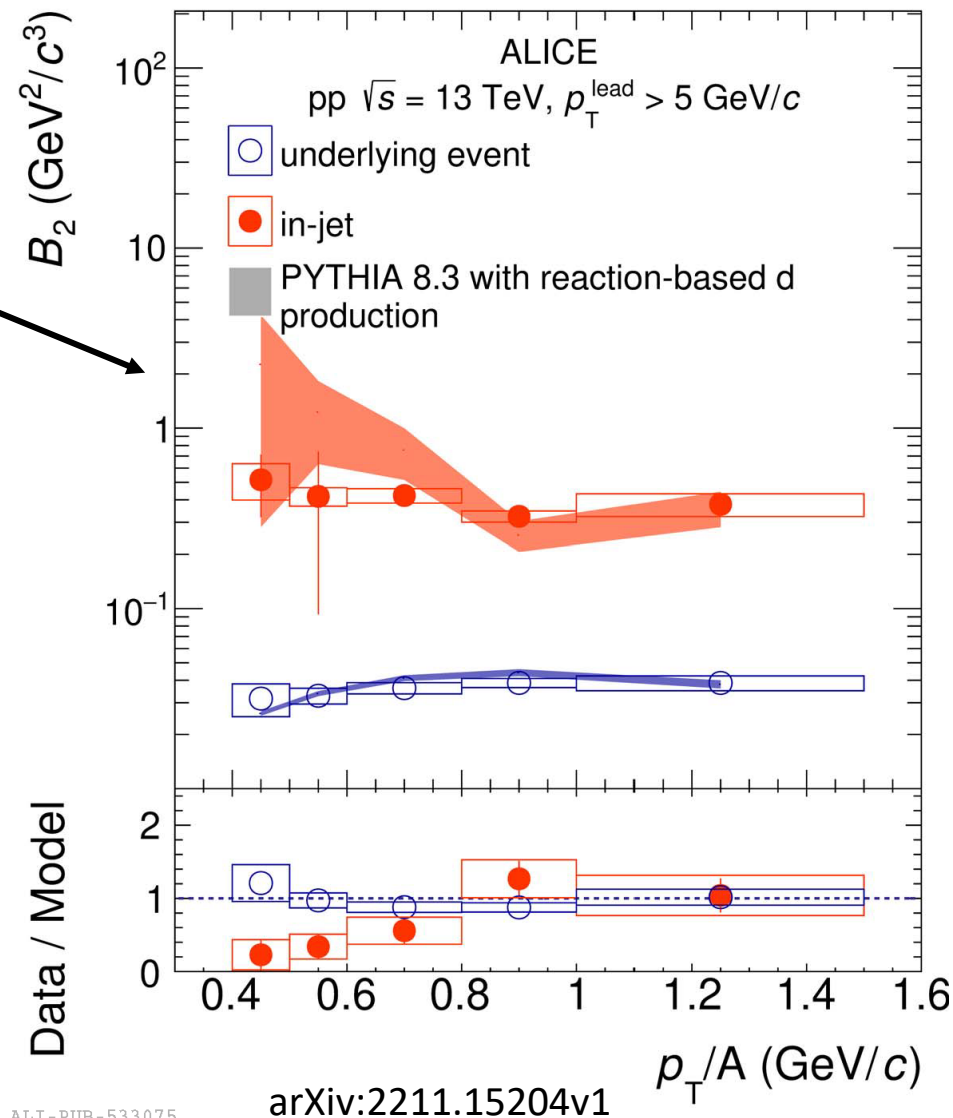
- Two different models:
  - PYTHIA 8 Monash 13 + simple coalescence
  - PYTHIA 8.3 with reaction-based deuteron production (Bierlich et al., arXiv:2203.11601)
- Both models qualitatively reproduce the data and the large difference between  $B_2^{\text{jet}}$  and  $B_2^{\text{UE}}$



# $B_2$ in jet and UE – model comparison



- Two different models:
  - PYTHIA 8 Monash 13 + simple coalescence
  - PYTHIA 8.3 with reaction-based deuteron production (Bierlich et al., arXiv:2203.11601)
- Both models qualitatively reproduce the data and the large difference between  $B_2^{\text{jet}}$  and  $B_2^{\text{UE}}$
- Further comparison with models



# Summary

---

- Light (anti)deuteron production in three azimuthal regions in pp and p–Pb collisions
- Coalescence parameter in-jet and underlying event
  - Enhancement of  $B_2^{\text{jet}}$  wrt  $B_2^{\text{UE}}$  of a factor 15 (24) in pp (p–Pb) collisions
- **Higher  $B_2^{\text{jet}}$  in p–Pb collisions wrt pp collisions**
  - **Nucleons are probably closer in momentum space in p–Pb wrt pp**
- **Higher d/p ratio in p–Pb collisions wrt pp collisions for jets**
- Good agreement with model comparison in pp collisions
- New investigation in Run 3 data

Thank you for the attention!

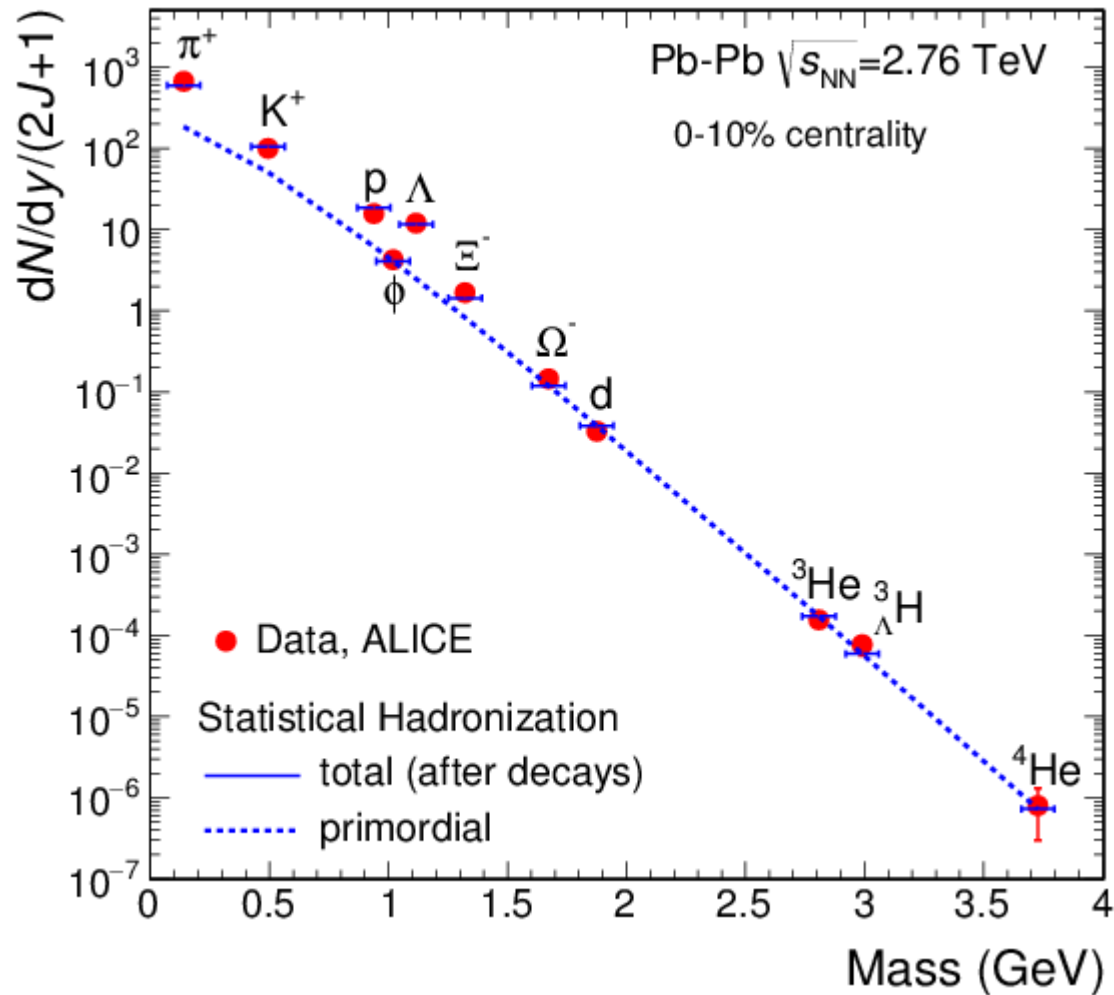


# Backup

---



# Statistical models



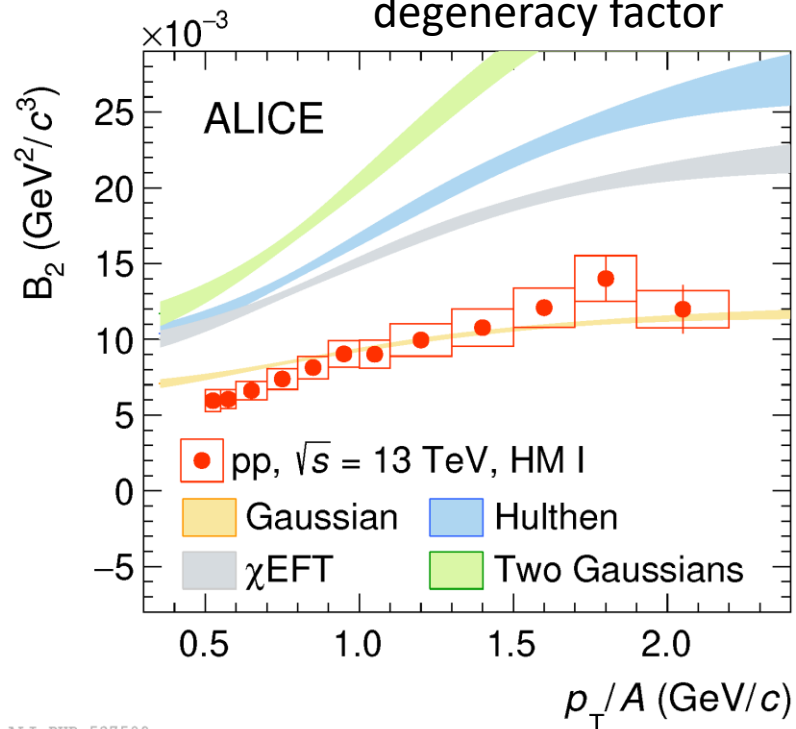
- Hadrons emitted from a system in statistical and chemical equilibrium
- $T_{\text{chem}}$  is the key parameter
- $dN/dy \propto \exp(-m/T_{\text{chem}})$
- Nuclei binding energy  $\sim$  few MeV  $\rightarrow$  how they can survive?
- Particle yield well described with a common  $T_{\text{chem}}$  of  $\sim 156$  MeV

Andronic et al, Nature vol. 561, 321-330 (2018)

# (Advanced) coalescence model

- Wigner function formalism

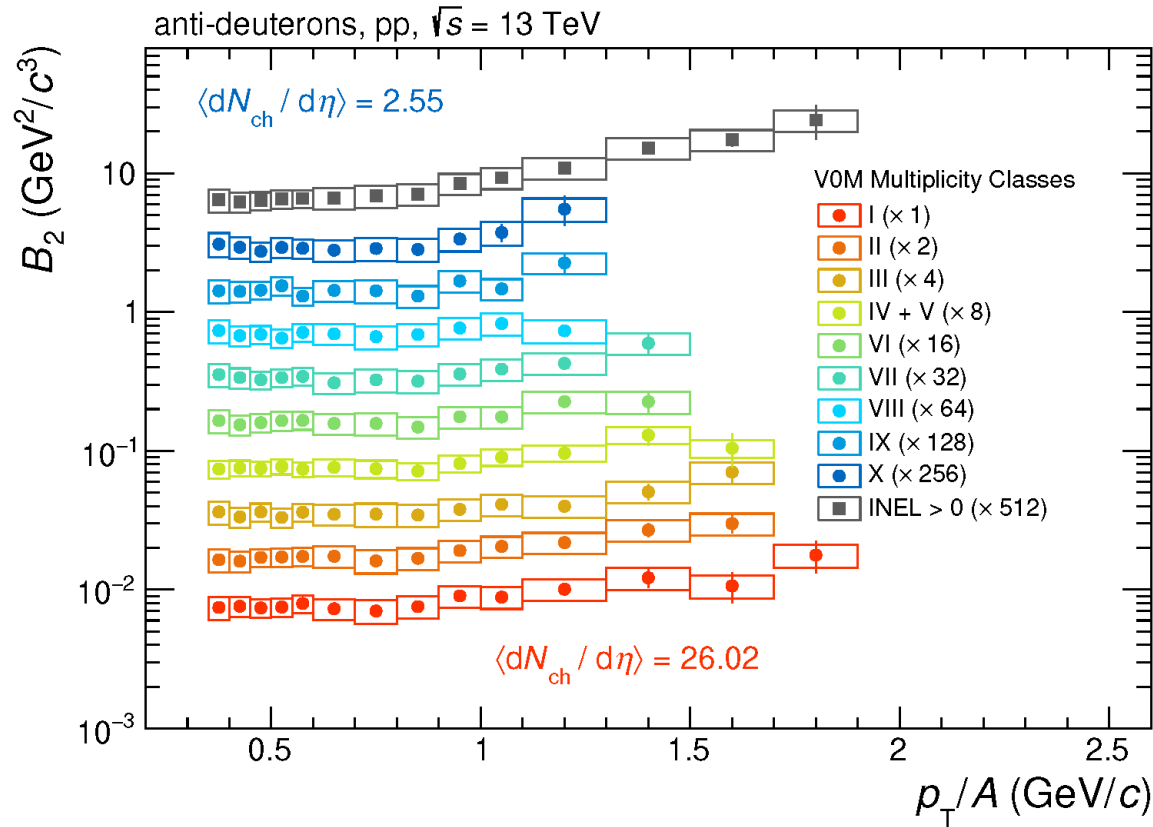
$$N_A = \underbrace{g_a}_{\text{spin-isospin degeneracy factor}} \cdot \int d^3x_1 \dots d^3x_A \cdot \underbrace{d^3k_1 d^3k_A \cdot f_1(x_1, k_1) \cdot f_A(x_A, k_A)}_{\text{phase space distributions of nucleons}} \cdot \underbrace{W_A(x_1, \dots, x_A, k_1, \dots, k_A)}_{\text{Wigner density of nucleons}}$$



- Different Wigner density functions available:

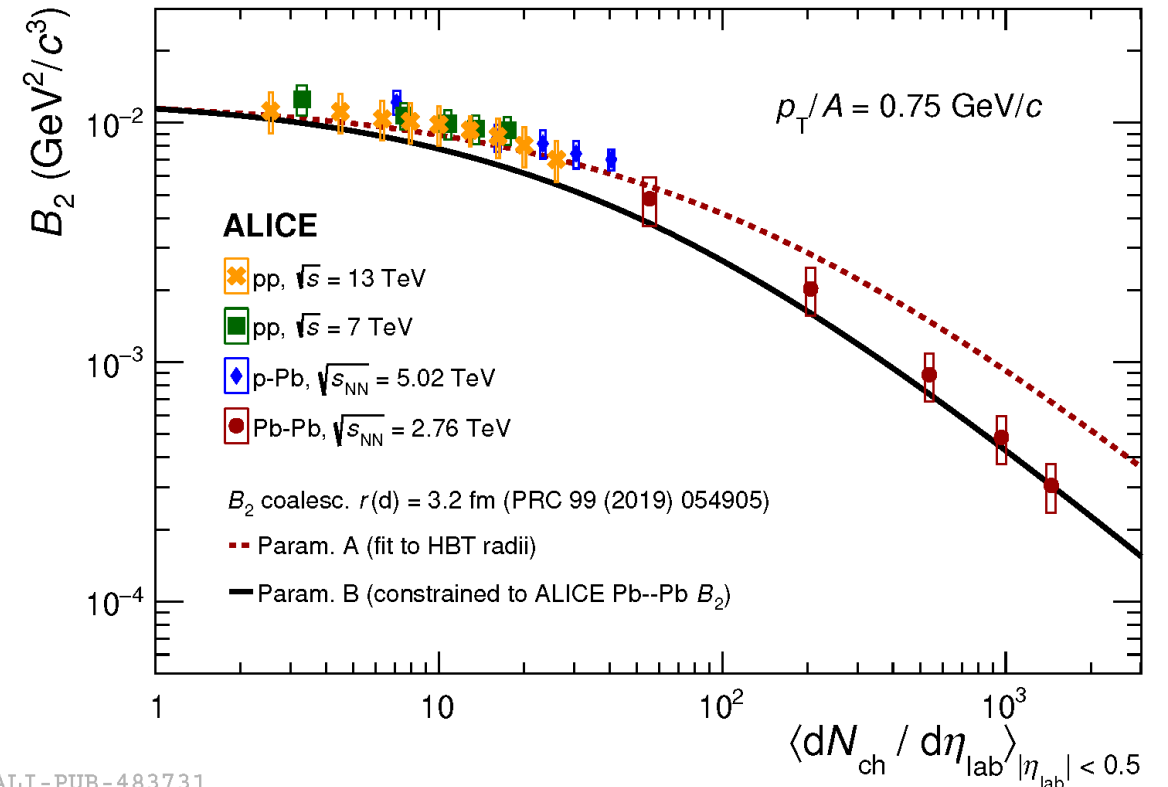
- Gaussian: standard one
- Double gaussian
- Hulthén: Yukawa-like potential
- $\chi$ EFT: Chiral effective field theory

JHEP 01 (2022) 106



ALI-PUB-483726

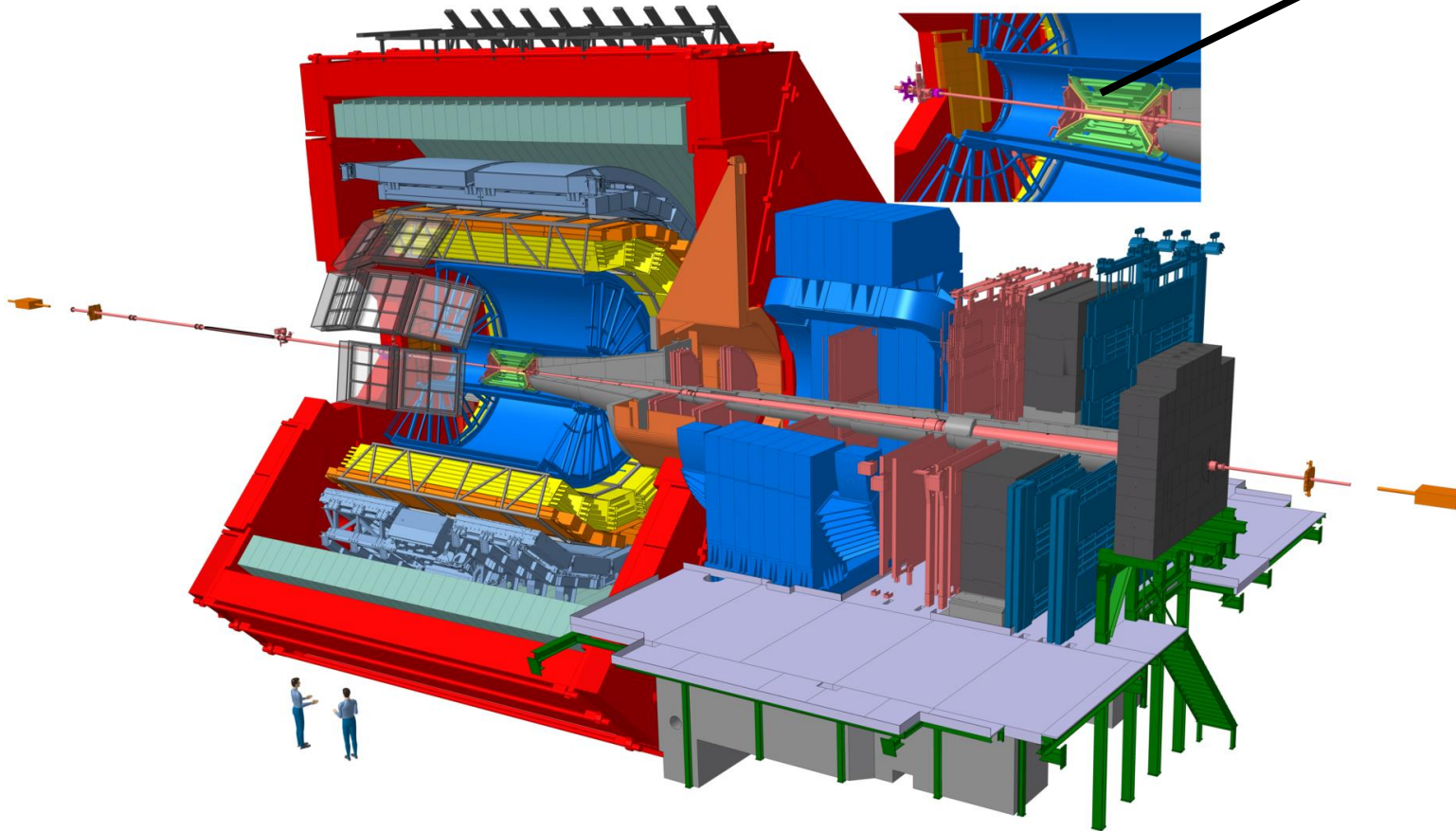
- $B_A$  is rather flat in all multiplicity classes, but increase at high  $p_T/A$  in the MB class



ALI-PUB-483731

- Smooth evolution from small to large source size

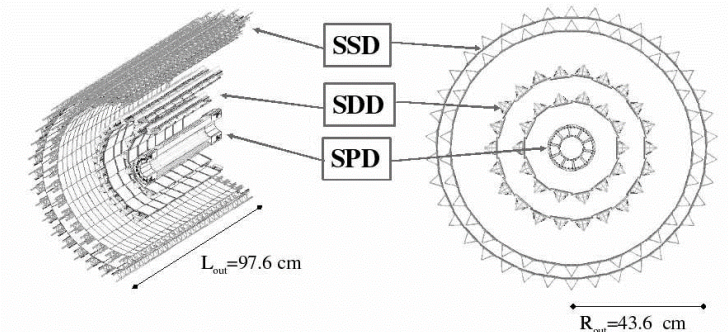
# The ALICE detector in Run 2



## Inner Tracking System (ITS)

Six concentric layer of silicon sensors:

- 2 layers of Silicon Pixel Detectors (SPD);
- 2 layers of Silicon Drift Detectors (SDD);
- 2 layers of Silicon micro-Strip Detectors (SSD).

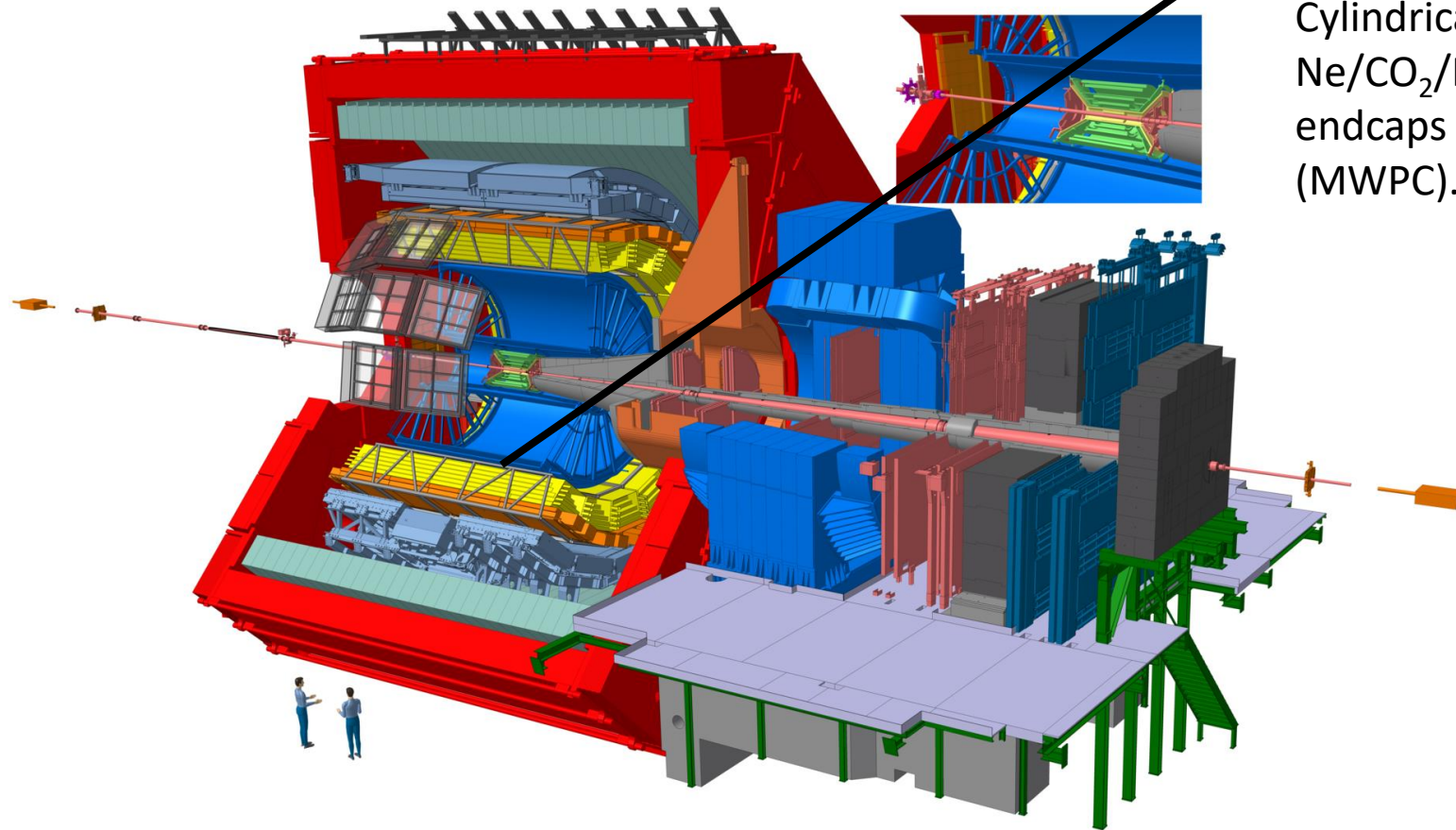


*JINST* 3 (2008) S08002

Int. J. Mod. Phys. A 29 (2014) 1430044

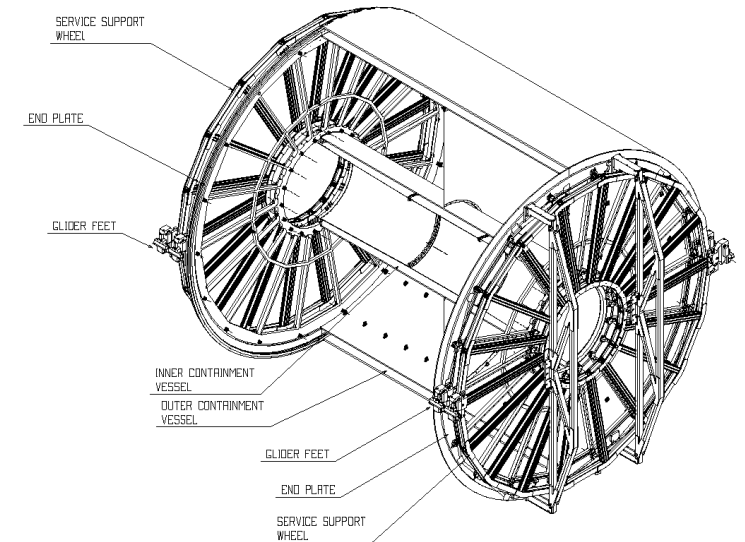


# The ALICE detector in Run 2



## Time Projection Chamber (TPC)

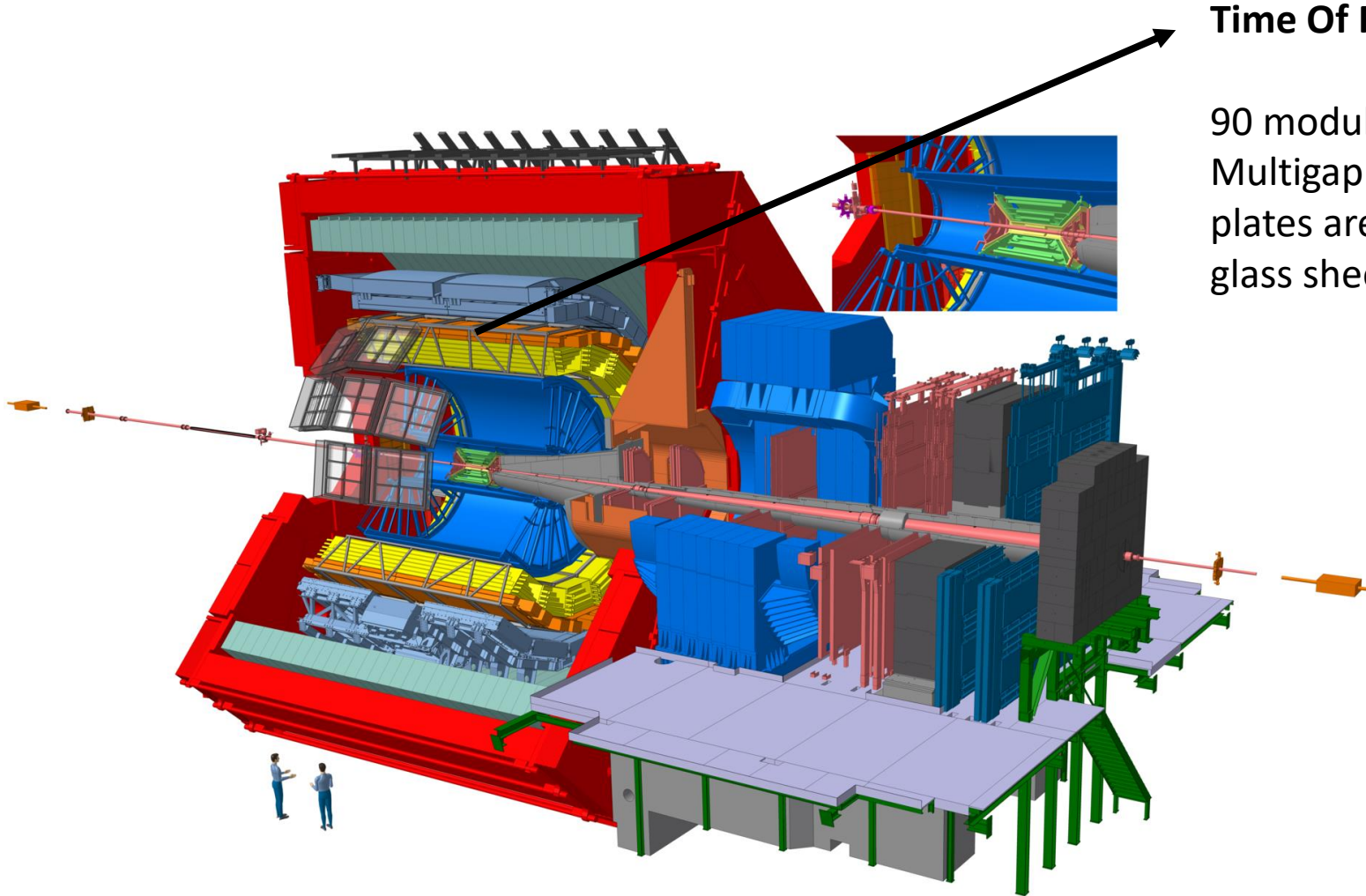
Cylindrical gas detector, made by a field cage filled with Ne/CO<sub>2</sub>/N<sub>2</sub> (90/10/5). The cage is closed with two endcaps made of Multi-Wire Proportional Chambers (MWPC).



JINST 3 (2008) S08002

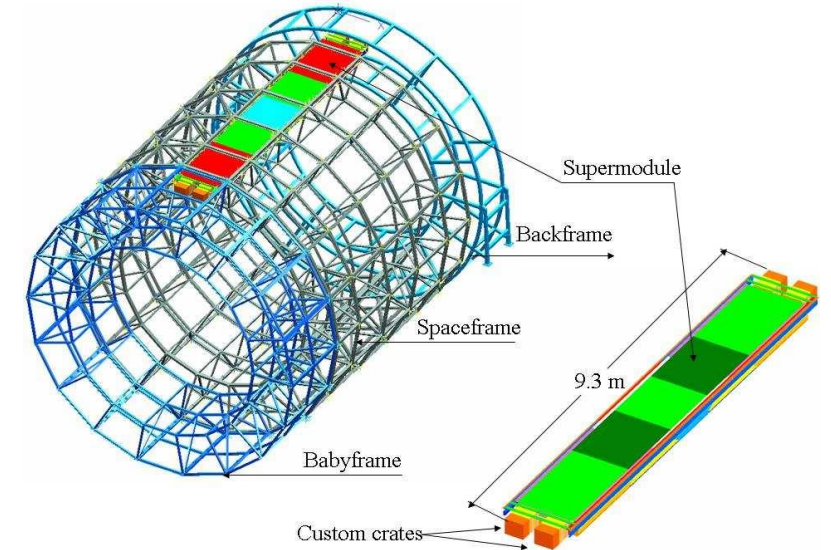
Int. J. Mod. Phys. A 29 (2014) 1430044

# The ALICE detector in Run 2



## Time Of Flight (TOF)

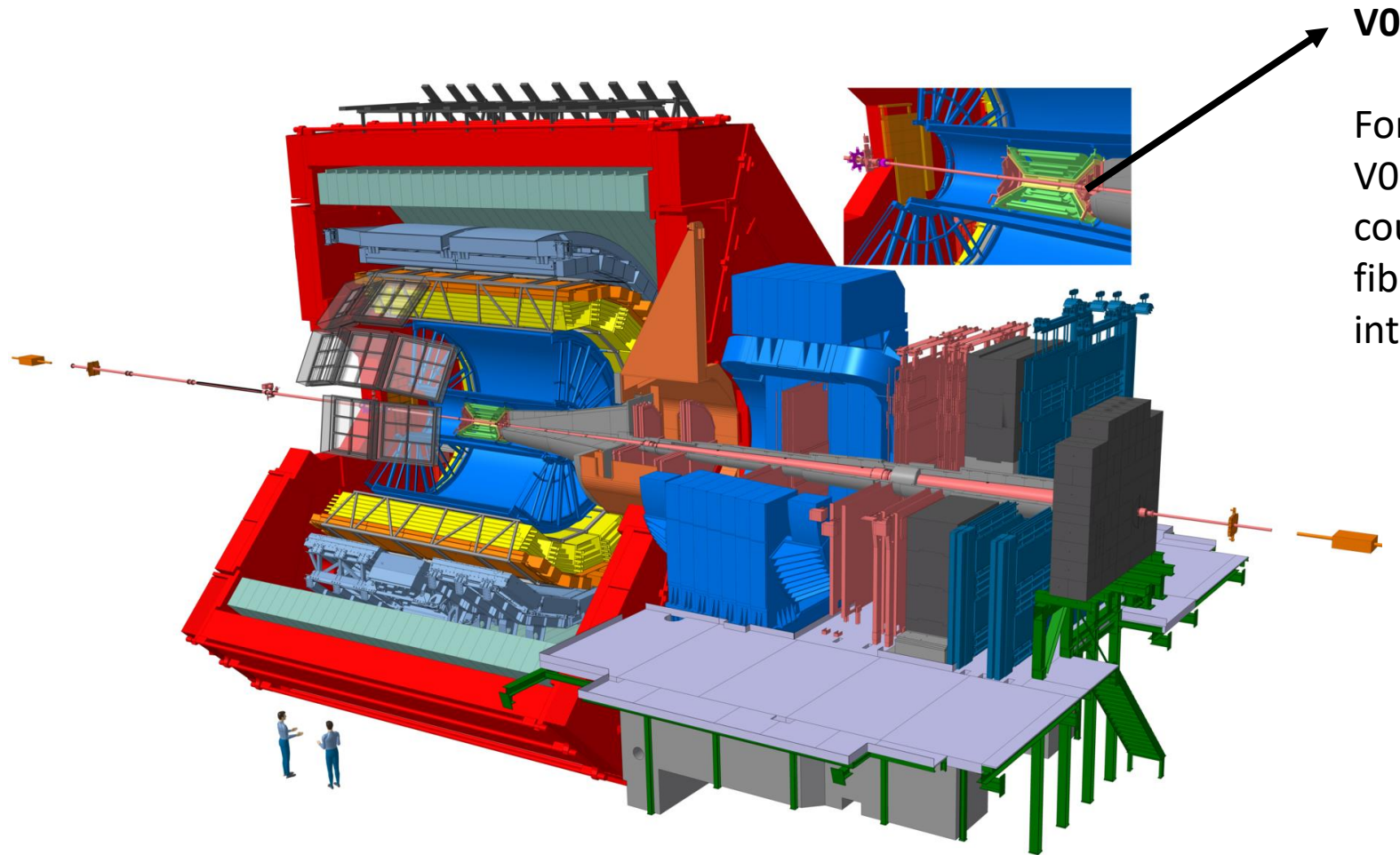
90 modules formed by a system of 10 gaps double stack Multigap Resistive Plate Chambers (MRPC). The resistive plates are made with commercially available soda-lime glass sheets with a gap of  $250 \mu\text{m}$ .



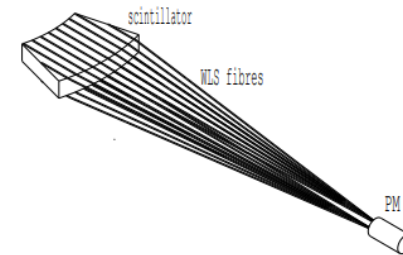
*JINST* 3 (2008) S08002  
Int. J. Mod. Phys. A 29 (2014) 1430044



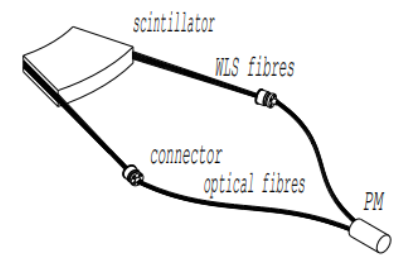
# The ALICE detector in Run 2



Formed by two different modules, VOA and VOC, consisting of two arrays of scintillator counters and Wave-Length Shifting (WLS) fibres installed on either sides of the interaction point.



VOA



VOC

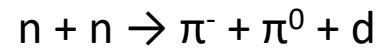
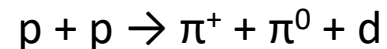
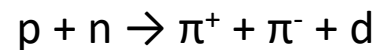
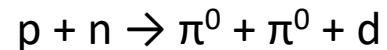
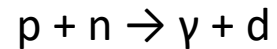
*JINST* 3 (2008) S08002

Int. J. Mod. Phys. A 29 (2014) 1430044

- PYTHIA 8.3:

- d production via ordinary reactions
- Energy dependent cross sections parametrized based on data

- Reactions:



- PYTHIA 8 Monash:

- Simple coalescence
- d is formed if  $\Delta p < p_0$ , with  $p_0 = 285 \text{ MeV}/c$